8-31-2016

Examining Valve Shape Variation in the Freshwater Diatom Genus Eunotia over Time and Space

Jordan M. Bishop
University of Connecticut - Storrs, jordan.bishop@uconn.edu

Examining Valve Shape Variation in the Freshwater Diatom Genus *Eunotia* over Time and Space

Jordan Bishop

B.A., Connecticut College, 2014

A Thesis

Submitted in Partial Fulfillment of the

Requirements for the Degree of

Master of Science

At the

University of Connecticut 2016

2016

APPROVAL PAGE

Masters of Science Thesis

Examining Valve Shape Variation in the Freshwater Diatom Genus *Eunotia* over Time and Space

Presented by

Jordan Bishop, B.A.

Major Advisor Louise A. Lewis
Louise A. Lewis

Associate Advisor Paul Lewis
Paul Lewis

Associate Advisor Andrew M. Bush
Andrew Bush

Associate Advisor Peter D. Siver
Peter Siver

University of Connecticut

2016

Dedication

For Maurizio and Pietro Genovesi.

Acknowledgements

I'd like to thank the EEB department and my fellow graduate students for all their support, throughout both personal and professional endeavors.

Without the monetary support from The UConn graduate school, specifically the Multicultural Scholars Program, and EEB department, this research would have been much more costly and it is with the sincerest of gratitude that I thank them for their generosity. I thank the entire team behind the Multicultural Scholars Fellowship for always lending a helping hand, and feeding me during orientation, final exams and throughout the academic year.

I'd like to thank my committee for the guidance, and pushing, necessary to survive graduate school. I am especially grateful for the support of Dr. Louise Lewis and her lab of crack phycologists, who never hesitated to offer their support within all aspects of scholarly life.

Table of Contents

Chapter 1: Diatom morphometrics and its use to study the environment and in systematics

Introduction: As an important component of the base of the food chain within the world's oceans, diatoms are responsible for between 20-40% of the organic matter produced on an annual basis (Aude et al., 2015). All told, diatoms are responsible for approximately 20% of the globe's photosynthesis (references within Wolfe and Siver, 2009). They abound in both marine and freshwater ecosystems, so too within brackish environments. Diatoms are even known to occur within soil; some thrive in Polar Regions. Diatoms are placed within the heterokonts, also known as the stramenopiles, one of the major eukaryotic supergroups (Graham et al., 2009). A more complete discussion of diatom origins and their fossil record is provided in Chapter 2.

Valve Morphology: Diatoms possess a uniquely evolved frustule, or shell, composed entirely of silicon dioxide, or glass (Lee, 1992). It is within this frustule that the diatom lives. The diatom frustule consists of two overlapping valves connected by girdle elements, also referred to as girdle bands, or cingula. Valves may also be referenced by their respective positions within the frustule. The slightly larger epitheca rests upon the slightly smaller hypotheca. The thecae are comprised of a valve and cingula. Therefore, the epitheca comprises the epivalve and epicingulum while the hypotheca consists of the hypovalve and hypocingulum. Functionally, diatoms are composed of two overlapping petri dishes. The ring-like cingula serve to connect the two valves and often present as a number of hollow structures that are often associated with the epivalve or hypovalve, in which case they are referred to as the epicingulum and hypocingulum, respectively. Finally, the valve face is the outward facing portion of the valve. Continuing with the petri dish analogy, this is akin to the top and bottom portion of the petri dish. The valve mantle would be that portion of the valve, when viewed from the side, that is often in contact with the girdle bands. This would be the lip or edge of the petri dish, i.e., those surfaces

perpendicular to the flat "faces" of the petri dish. Once formed, the diatom frustule can expand by adding girdle bands, which move the valves further apart. Thus, the valve face does not change in size; only girth is added to the frustule. Diatoms exhibit a gradual decrease in size from generation to generation as the product of mitotic division (implications of this phenomenon for taxonomy are addressed in Chapter 2).

Ecology: These single-celled organisms generally occur as solitary cells, though colonial and filamentous forms are present as well, filling niches in both planktonic and periphytic communities (Dodd, 1987). Despite their ability to grow within a wide range of environments, many species have restricted environmental tolerances. Some taxa prefer pristine, oligotrophic waters, while others thrive in acidic or eutrophic waters. As a whole they are noted for their rapid response to environmental change and stress (Brazner et al., 2007). It is for this reason that diatoms have been used as bioindicators, since particular suites of species, and even genera, can be distributed across an enormous span of environmental gradients (Wehr and Sheath 2003). Additionally, the preserved siliceous remains of diatoms are extensively used as proxy data for paleoreconstructions of past freshwater and marine environments (Jiang et al., 2001; Verleyen et al., 2004; Abrantes and Moita 2007; Yang et al., 2008).

Morphological Methods in Diatoms: Both discrete and continuous characters are used to determine diatom identity. As resolution improved with microscopy, so did the ability of diatomists to further resolve the overall structure within diatoms. Using light microscopy, valve length and width measures are recorded first. These measures are recorded with the diatom valve in valve view. Striations, or striae, occurring along the valve are recorded as the number per 10 microns, often measured at the valve center. Striae are also often qualitatively described in terms of the pattern and orientation along the different segments of the valve, such as near the apices

compared to the center or margins (Hansmann, 1973). Length, width and striae density are often presented as ranges alongside a size declination series of photographs that show the overall change in valve morphology within a species population (Metzeltin and Lange-Bertalot, 1998). Although most structures can be identified using light microscopy, electron microscopy allows further investigation of the finer ultrastructure of the frustule. It has proven especially helpful in providing details for cryptic structures, namely raphes (Siver et al., 2011) and thusly has aided to rework taxonomy. Electron microscopy has also helped to determine the size and morphology of the pores that comprise the striae, namely occluding structures such as hymenes. Most often, a combination of light and electron microscopy are used in tandem for verifying taxonomy. Many characters are also used by diatomists to delineate (and identify) species, such as the presence or absence of a raphe, details in girdle view (especially planes of symmetry), spines or other projections emanating from the frustule surface, and shape and curvature of valve apices and margins.

Valve Morphology & Taxonomy: Classically, valve shape, as well as its symmetry, has been used to define the three large clades within diatoms. However, save for agreement upon the higher taxonomic nomenclature, the classic literature is rife with a dizzying array of taxonomic schemes. A number of these were compiled and compared within Patrick and Reimer's tome, *The Diatoms of North America* (1966). Their two volumes laid the groundwork for the canonization, arguably, of diatom taxonomy with Round et al. (1990). The classic definitions of centric and pennate diatoms were incorporated into the nomenclature, with a further distinction made between the raphid and araphid pennate diatoms within Round et al. (1990). Under Phylum Bacillariophyta, three large classes are Coscinodiscophyceae, Fragilariophyceae, and Bacillariophyceae. These classes correspond to the centric diatoms, araphid pennate, and raphid

pennate diatoms, respectively. Additionally, a number of subclasses and orders were proposed. The work of Round et al. (1990) is more concerned with providing a tool to be utilized by researchers. Genera are described using internal and external morphological characters, with a noted absence of measures of continuous traits. This was deliberate, as Round et al. (1990), state that diatoms exhibit a large amount of both inter- and intraspecific variation. Notably favoring morphological taxonomy, Round et al. (1990), acknowledge the emerging use of molecular data within diatom systematics. Moving beyond Round et al. (1990), work has been undertaken to improve resolution of diatom taxonomy using molecular systematics, though only a handful of genera have been thoroughly studied so far.

Molecular Methods & Taxonomy: Molecular methods have improved the overall understanding of diatoms, especially within the larger clades. Medlin et al. (1993) showed that the centric and araphid pinnate diatoms might not be monophyletic using maximum parsimony and distance matrices to investigate ribosomal 18S rRNA data in conjunction with records of fossil taxa. Sims et al. (2006) compiled literature that improved understanding of the diatoms as a group, with careful consideration of molecular, morphological and fossil data. Most notably, Medlin and Kaczmarska (2004) present an alternative classification scheme based upon molecular and morphological data uncovering polyphyly within the three classes proposed by Round et al. (1990). The study analyzed a total of three datasets of ribosomal RNA genes; two included the 18S (nuclear) gene while the third investigated the16S (plastid) gene. The first 18S and sole 16S datasets were analyzed using a maximum parsimony (MP) with bootstraps. The second 18S dataset were analyzed using maximum likelihood (ML) and neighbor joining (NJ), using a general time reversal (GTR) model of evolution. This same 18S dataset was used again for Bayesian inference (BI). These data were coupled with cytological evidence including Golgi

body arrangement, auxospore development, and ultrastructural investigation of pyrenoid and spermatozoids. These combined analyses led Medlin and Kaczmarska (2004) to propose a revised classification more accurately reflecting evolutionary relationships, i.e., those not present within the classification scheme proposed by Round et al. (1990). Medlin and Kaczmarska (2004) incorporated the scheme of Round et al. (1990) yet shifted component members around based upon their findings to propose two subdivisions, Coscinodiscophtina Medlin and Kaczmarska, 2004 and Bacillariophytina Medlin and Kaczmarska, 2004. Further changes were a single class Coscinodiscophyceae Round & Crawford, emend. Medlin and Kaczmarska under the former subdivision, with two classes under the latter: Mediophyceae (Jousé & Proshkina-Lavrenko) Medlin and Kaczmarska, 2004 and Bacillariophyceae Haeckel, emend. Medlin and Kaczmarska, 2004. This revised classification differs from that of Round et al. (1990) in that the centric diatoms are separated into two classes and the pennates grouped into a single class. The first, Coscinodiscophyceae, contains centric diatoms with radial symmetry. The second class, Mediophyceae, features the bipolar and multipolar centrics and the radial centric Thalassiosirales. The Bacillariophyceae features the combination of both raphe and nonraphe bearing pennate diatoms. Medlin and Kaczmarska (2004) demonstrated that although resembling other centric diatoms morphologically, the Thalassiosirales is more closely aligned phylogenetically with the pennates than with other centrics.

Despite the proposed revisions of Medlin and Kaczmarska (2004), Round et al. (1990) is used still as the classification scheme most often employed; it was devised as a means of organizing and describing the genera and was not meant to accurately represent neither phylogenetic relationships nor how the genera evolved (Sims et al., 2006). Currently, molecular methods are used to investigate generic and species-level descriptions, though this too has seen

limited practice (Poulíčková et al., 2010). Mostly studies have investigated cryptic species complexes, or to inform more small-scale phylogenetic relationships among related taxa (Souffreau et al., 2011). Target genes for diatom phylogenies, and barcoding, have aimed at the chloroplast, nuclear and ribosome yet results are largely dependent upon the gene examined as well as the taxon studied (Macgillivary et al., 2011; Luddington et al., 2012). There is also a marked lack of specific primers for a number of genes (Moniz and Kaczmarska, 2009; Guo et al., 2015). As particular markers show favorable results, those are utilized to examine the genetic basis of ecological roles. Nakov et al. (2014) used ordinal-level diversity to examine the evolutionary history of planktonic and colonial growth forms and their relationship with niches within the plankton or benthos. The study by Nakov et al. (2014) generated a tree based on previous and new sequence data using three genes, ribosomal SSU, rbcL and psbC. For now, this is the trend within the diatoms as there is no larger agreed upon phylogeny for the group. Among other reasons, this is due in part to the tremendous number of species thought to exist within the diatoms.

Round et al. (1990) did not enumerate a count for species within their description of the genera, but indicated the difficulty in diatom systematics with regards to the adoption of species concepts. In particular, deciding upon which species concept, i.e. morphological, molecular, fossil, among others, to use given the overwhelmingly large amount of diatom species and inconsistent coverage of sampling (1990). Sims et al. (2006) followed a similar path, but instead noted the difficulty in discerning species boundaries. Here, although morphological data can be imprecise, molecular data may be ameliorating the fight. As it stands, around 2% sequence divergence is where the cutoff for diatom species, though this too is up for debate (Guo et al., 2015). Time and again, the oft cited Mann and Vanormelingen (2013) work gives a wide range;

from about 30,000 to 100,000 species. They also are quick to note that there are still regions of the world from which there has been little to no sampling. Theriot et al. (2011) further posit that there is limited agreement upon trees and methods used to compile them, as well as sampling bias within clades. Overall, a well analyzed phylogeny for the diatoms will depend on concerted work pursuing this goal using established methods, such as morphometrics, and pairing them with the molecular methods still gaining a foothold within diatom systematics (William and Kociolek, 2010). Morphometrics has proven especially useful in species-level systematics where sequence data may not be practical or available, in particular, with detailing species boundaries amongst morphospecies (Fránková et al., 2009). Geometric morphometrics can also be used to compare fossil specimens amongst each other, and may be used to extend this comparison to include extant taxa (Kotrc and Knoll, 2015). A number of diatom genera, would fit this criterion, including *Eunotia*.

Generic Descriptions: The focal genus in this study is *Eunotia* C.G. Ehrenberg 1837. Following the classification of Round et al. (1990), this species-rich genus is placed within the Bacillariophyceae Haeckel 1878, a member of subclass Eunotiophycidae D.G. Mann 1990, and order Eunotiales Silva 1962. Within the order, two families Peroniaceae (Karsten) Topachevs'kyj & Oksiyuk 1960 and Eunotiaceae Kützing 1844, are recognized. *Peronia* A. de Brebisson & G.A.W. Arnott ex F. Kitton 1868 is the sole genus within Peroniaceae, whereas the diverse Eunotiaceae contains the genera *Desmogonium* Ehrenberg 1848*, Actinella* F.W. Lewis 1864*, Semiorbis* R. Patrick 1966 and *Eunotia*. Additional genera have been added since Round et al. (1990): *Eunophora* W. Vyverman, K. Sabbe & D.G. Mann 1998*, Amphorotia* G.M. Williams & G. Reid 2006 and *Perinotia* D. Metzeltin & H. Lange-Bertalot 2007*, Eunotioforma* J.P.Kociolek & A.L.Burliga, 2013, *Amphicampa* (C.G. Ehrenberg) Ralfs, 1861,

Colliculoamphora D.M. Williams & G. Reid 2006, and *Bicudoa* C.E. Wetzel, H.Lange-Bertalot & L. Ector 2012 (Vyverman et al., 1998; Williams and Reid 2006; Ferrari et al., 2009; Harper et al., 2009; Guiry and Guiry, 2015; Fourtanier and Kociolek, 2015).

Eunotia is asymmetrical about the apical axis, with valve apices bent to one side, giving the valve a banana-like, or even semi-lunate appearance. The concave, ventral margin is shorter and often smooth. The dorsal margin is often convex, with certain taxa displaying ornamentations such as gentle undulations, or waves, to numerous, distinct projections, often called "humps." *Eunotia* has a raphe with the distal end of the raphe structure terminating upon the valve face or nearly so; specifically, the junction of the mantle and aforementioned valve face. Raphe slits are reduced within *Eunotia*, restricted to the valve apices and situated predominantly on the valve mantle, which lacks central nodules. This condition is distinct within raphe bearing diatoms, as raphes are most often observed entirely upon the valve face. Internally, a thickened helictoglossal is associated with the distal raphe fissure. Rimoportulae are featured internally within the apices of the valve. These structures, when present, occur one per valve and may oppose one another within the hypovalve and epivalve. Few taxa lack them completely, while in other instances a taxon may possess more than one. Striae are small, uniseriate poroids lacking hymenes or other occlusions. The genus features near cosmopolitan distribution, with the vast majority of species restricted to freshwater systems. No less than 500 species of *Eunotia* have been described (Kulikovskiy et al., 2015). Fossil records indicate that the genus was established as early as the Eocene, where it has been seen to co-occur with other members of the Eunotiales, most notably *Actinella* (Siver et al., 2010, 2015).

Morphometrics: Traditionally, morphometrics allowed the covariation of shape patterns alongside a trait of interest, such as length, width, or height. Measures of these morphological

traits were often linear distances, though angles and ratios of two, or more, measures were also quantified. From these, multivariate analyses were performed (Claude, 2009). However, these traditional morphometric approaches often lacked the ability to convey information about the shape of the object under study. The details associated with shape, and their relationships to the linear measures, could not be graphically displayed and interpreted as one. A variety of approaches throughout the 1980's led to alternative methods that preserved the shape component within the morphological measures. A more modern approach, Geometric Morphometrics, allows for the retention of shape data alongside linear measures of morphological traits, though shape data are independent of size when measured using this approach (Adams et al., 2004; Adams et al., 2013). Historically, this was accomplished first through outline methods, which quickly led to the landmark methods (Pappas et al., 2014). Here, I will describe a specific landmark method based upon two-dimensional permanent and semi-permanent landmarks, as it is the most pertinent to our discussion of morphometrics. However, although not applicable to this study, there are also a plethora of methods for three-dimensional analyses.

Landmark analysis within Geometric Morphometrics: In this study, landmarks denote biologically important structures or positions. Fixed, or permanent, landmarks anchor the semi-permanent, or sliding, landmarks. The semi-permanent landmarks are used to capture the smaller variances in shape between the fixed, or permanent, landmarks. Though the available software, semi-landmarks are "slid" into place, becoming evenly spaced between the anchored fixed landmarks. This aids to reduce error and potential bias introduced into the analysis by tiny deviations in placement of the landmarks, minimizing the shape difference between specimens (Bookstein, 1997; Adams et al., 2004). After landmarks are placed, multivariate statistics can be performed. Finally, shape variation can be graphically displayed, most often through ordination

analyses such as a principal components analysis (PCA) with, or separately from, a thin-plate spline transformation grid that can allow for visual comparison between specimens, displaying landmarks and their resultant outline (Rohlf, 2002).

Diatom Taxonomy & Early Geometric Morphometrics: The utility of traditional morphometrics has been long understood within the diatoms, as nearly every study examining the diatoms contains linear measurements such as length and width accompanying qualitative descriptions of valve characteristics. Chief among these are descriptions of the valve morphology that characterize the linear measures, such as ornamentations of the valve, convexity/concavity, alongside presence/absence of the raphe, striations and other morphologically relevant traits (Siver and Hamilton, 2011). The quantification of the size differences, due in part to the size declination, range within a single species population, as well as the overlap in the size series of multiple taxa, necessitates a way to compare measurements alongside valve shape morphology; this has been known for some time (Geitler, 1932; Patrick and Reimer, 1966). Stoermer and Ladewski (1982) introduce the idea of "sorting" alongside traditional morphometrics, through Legendre polynomials, as a way of quantifying the observed differences in shapes amongst type and modern material of *Gomphonema herculeana* (Ehrenberg). Using the outline method of geometric morphometrics, this study highlighted the difficulty of using the outline method for extracting valve shape outline within ontogenetic growth series. However, landmark analysis, more specifically landmark analysis that included both permanent and semi-permanent landmarks, has been since widely utilized within pennate diatoms.

Geometrics Morphometrics & *Eunotia*: Morphometrics provides a valuable tool to examine *Eunotia* systematics because the genus lacks a molecular phylogenetic tree. Only about 5 species sequences exist alongside multiple strains available on NCBI GenBank (accessed 12/14/15).

However, *Eunotia* has extensive fossil records dating to the Eocene Epoch. In particular, the Giraffe Pipe sediment core features lacustrine deposits representing some of the oldest freshwater representatives of *Eunotia*, with fossils suggesting that the morphology of the genus was established as early as 40Ma and have persisted since that time (Siver and Wolfe, 2007). Using geometric morphometrics landmark analyses, fossil taxa from the Giraffe Pipe locality were shown to be significantly different when compared against extant North American and European taxa. The valve shapes of fossil taxa were generally more conserved, and composed a subset of their modern counterparts. The latter features a larger range of valve shape morphology than what is thought to exist within the fossil record (Bishop-Genovesi, 2014). Using similar methods of landmark based shape analysis, alongside ecological data, English and Potapova (2012) identified separate shape groups and removed two species from synonymy. Once again, landmark methods used in tandem with type specimens have the ability to uncover morphospecies (Fránková et al., 2009). Geometric morphometrics can inform phylogenetics as well, though these methods have been sparsely applied and are limited to parsimony and maximum likelihood (Rohlf, 2002; Adams et al, 2013). The following chapter builds on Bishop-Genovesi (2014) using an expanded dataset of modern and fossil taxa, with special consideration given to type materials and tropical specimens. The goal is to characterize the shape variation within *Eunotia* with respect to its ecology and geography across a temporal gradient while demonstrating the resolving power of a geometric morphometrics study at the genus level.

References

Abrantes F and Moita MT. 1999. Water column and recent sediment data on diatoms and coccolithophorids, off Portugal, confirm sediment record of upwelling events. Oceanologica Acta 22(1): 67-84.

Adams DC, Rohlf FJ, Slice DE. 2013. A field comes of age: Geometric morphometrics in the 21st century. Hystrix, the Italian Journal of Mammalogy 24(1): 7-14.

Adams DC, Rohlf FJ, Slice DE. 2004. Geometric morphometrics; ten years of progress following the 'revolution'. Hystrix, the Italian Journal of Zoology 71(1): 5-16.

Aude B, Karen S, Benoît S. 2015. Editorial: Recent progress in diatom's taxonomy and freshwater ecology. Cryptogamie, Algologie 36(3): 241-44.

Bishop-Genovesi J. 2014. Evaluating trends in valve shape in *Eunotia* by comparing fossil and modern species. Undergraduate Thesis. New London: Connecticut College.

Bookstein FL. 1997. Landmark methods for forms without landmarks: Morphometrics of group differences in outline shape. Medical Image Analysis 1(3): 225-43.

Brazner J, Danz N, Niemi G, Regal R, Trebitz A, Howe R, Hanowski J, Johnson L, Ciborowski J, Johnston C. 2007. Evaluation of geographic, geomorphic and human influences on great lakes wetland indicators: A multi-assemblage approach. Ecological Indicators 7(3): 610-35.

Claude J. 2008. Morphometrics with R. Springer. 317 p.

Dodd J. 1987. Diatoms. The illustrated flora of Illinois. First ed. United States: Southern Illinois University Press. 478 p.

English JD and Potapova MG. 2012. Ontogenetic and interspecific valve shape variation in the Pinnatae group of the genus *Surirella* and the description of *S. lacrimula* sp. nov. Diatom

Research 27(1): 9-27.

Ferrari F, Wetzel CE, Ector L, Blanco S, Cerqueira Viana JC, Mendes da Silva E, de Campos Bicudo D. 2009. *Perinotia diamantina* sp. nov. , a new diatom species from the Chapada Diamantina, northeastern Brazil. Diatom Research 24(1): 79-100.

Catalogue of Diatom Names, California Academy of Sciences, On-line Version [Internet]; c2015 [cited 2015 December 12]. Available from:http://research.calacademy.org/research/diatoms/names/index.asp.

Fránková M, Ková AP, Neustupa J, Pichrtová M, Marvan P. 2009. Geometric morphometrics-a sensitive method to distinguish diatom morphospecies: A case study on the sympatric populations of *Reimeria sinuata* and *Gomphonema tergestinum* (Bacillariophyceae) from the river Bečva, Czech Republic. Nova Hedwigia 88(1-2): 81-95.

Geitler L. 1932. Der Formweschel der pennaten Diatomeen (Kieselalgen). Arch. Prostistenk. 78: 1-226. Germany.

Graham LE, Graham JM, Wilcox LW. 2009. Algae. Second ed. United States: Pearson. 616 p.

Guo L, Sui Z, Zhang S, Ren Y, Liu Y. 2015. Comparison of potential diatom 'barcode' genes (the 18S rRNA gene and ITS, COI, rbcL) and their effectiveness in discriminating and determining species taxonomy in the Bacillariophyta. International Journal of Systematic and Evolutionary Biology 65(Pt 4): 1369-80.

Hansmann EW. 1973. Diatoms of the streams of eastern Connecticut. Connecticut Geological and Natural History Survey, Bulletin #106. 119 p.

Harper MA, Mann DG, Patterson JE. 2009. Two unusual diatoms from New Zealand: *Tabularia variostriata* a new species and *Eunophora berggrenii*. Diatom Research 24(2): 291-306.

Jiang H, Seidenkrantz M, Knudsen K, Eirıksson J. 2001. Diatom surface sediment assemblages

around Iceland and their relationships to oceanic environmental variables. Marine Micropaleontology 41(1): 73-96.

Kotrc B and Knoll AH. 2015. A morphospace of planktonic marine diatoms. I. Two views of disparity through time. Paleobiology 41(01): 45-67.

Kulikovskiy M, Lange-Bertalot H, Witkowski A, Khursevich GK, Kociolek JP. 2015. New species of *Eunotia* (Bacillariophyta) from lake Baikal with comments on morphology and biogeography of the genus. Phycologia 54(3): 248.

Lee RE. 1992. Phycology. Second ed. United States: Cambridge University Press.

Luddington IA, Kaczmarska I, Lovejoy C. 2012. Distance and character-based evaluation of the V4 region of the 18S rRNA gene for the identification of diatoms (Bacillariophyceae). Public Library of Science One 7(9): e45664.

MacGillivary ML and Kaczmarska I. 2011. Survey of the efficacy of a short fragment of the rbcL gene as a supplemental DNA barcode for diatoms. Journal of Eukaryotic Microbiology 58(6): 529-36.

Medlin LK and Kaczmarska I. 2004. Evolution of the diatoms: V. Morphological and cytological support for the major clades and a taxonomic revision. Phycologia 43(3): 245.

Medlin L, Williams D, Sims P. 1993. The evolution of the diatoms (Bacillariophyta). I. Origin of the group and assessment of the monophyly of its major divisions. European Journal of Phycology 28(4): 261-75.

Metzeltin D and Lange-Bertalot H. 1998. Tropische Diatomeen in Südamerika, I. Koeltz Scientific Books. Iconographia Diatomologica 5: 695 p.

Moniz MB and Kaczmarska I. 2009. Barcoding diatoms: Is there a good marker? Molecular Ecology Resources 9(s1): 65-74.

Nakov T, Ashworth M, Theriot EC. 2014. Comparative analysis of the interaction between habitat and growth form in diatoms. The ISME Journal. 9(1): 246-55.

Pappas JL, Kociolek JP, Stoermer EF. 2014. Quantitative morphometric methods in diatom research. Nova Hedwigia, Beiheft 143:281-306.

Patrick R and Reimer CW. 1966. The diatoms of the United States: Exclusive of Alaska and Hawaii. First ed. United States: Academy of Natural Sciences of Philadelphia. 688 p.

Poulíčková A, Veselá J, Neustupa J, Škaloud P. 2010. Pseudocryptic diversity versus cosmopolitanism in diatoms: A case study on *Navicula cryptocephala* Kütz. (Bacillariophyceae) and morphologically similar taxa. Protist 161(3): 353-69.

Rohlf FJ. 2002. Geometric morphometrics and phylogeny. Morphology, Shape and Phylogeny. 175 p.

Round FE, Crawford RM, Mann DG. 1990. The Diatoms: Biology & Morphology of the genera. First ed. United States: Cambridge University Press. 760 p.

Sims PA, Mann DG, Medlin LK. 2006. Evolution of the diatoms: Insights from fossil, biological and molecular data. Phycologia 45(4): 361-402.

Siver PA and Hamilton PB. 2011. Diatoms of North America: The freshwater flora of waterbodies on the Atlantic coastal plain. Gantner Verlag. Iconographia Diatomologica 22, 920 p.

Siver PA and Wolfe AP. 2007. *Eunotia* spp. (Bacillariophyceae) from middle Eocene lake sediments and comments on the origin of the diatom raphe. Botany 85(1): 83.

Siver PA, Bishop J, Lott A, Wolfe AP. 2015. Heteropolar eunotioid diatoms (Bacillariophyceae) were common in the North American arctic during the middle Eocene. Journal of Micropalaeontology 34(2): 151-63.

Souffreau C, Verbruggen H, Wolfe AP, Vanormelingen P, Siver PA, Cox EJ, Mann DG, Van de Vijver B, Sabbe K, Vyverman W. 2011. A time-calibrated multi-gene phylogeny of the diatom genus *Pinnularia*. Molecular Phylogenetics and Evolution 61(3): 866-79.

Stoermer EF and Ladewski TB. 1982. Quantitative analysis of shape variation in type and modern populations of *Gomphoneis herculeana*. Nova Hedwigia 73: 347-86.

Theriot EC, Ruck E, Ashworth M, Nakov T, Jansen RK. 2011. Status of the pursuit of the diatom phylogeny: Are traditional views and new molecular paradigms really that different? In: The Diatom World. Seckbach J and Kociolek JP, editors. Springer. 119 p.

Verleyen E, Hodgson DA, Leavitt PR, Sabbe K, Vyverman W. 2004. Quantifying habitat‐specific diatom production: A critical assessment using morphological and biogeochemical markers in Antarctic marine and lake sediments. Limnology and Oceanography 49(5): 1528-39.

Vyverman W, Sabbe K, Mann DG, Kilroy C, Vyverman R, Vanhoutte K, Hodgson D. 1998. *Eunophora* gen. nov. (Bacillariophyta) from Tasmania and New Zealand: Description and comparison with *Eunotia* and amphoroid diatoms. European Journal of Phycology 33(02): 95-111.

Wehr JD andSheath RG. 2003. Freshwater algae of North America: Ecology and classification. Academic Press. 917 p.

Williams DM and Reid G. 2006. Fossils and the tropics, the Eunotiaceae (Bacillariophyta) expanded: A new genus for the upper Eocene fossil diatom *Eunotia reedii* and the recent tropical marine diatom *Amphora reichardtiana* European Journal of Phycology 41(2): 147-54.

Williams DW and Kociolek JP. 2010. Towards a comprehensive diatom classification and

phylogeny (Bacillariophyta). Plant Ecology and Evolution 143(3): 265-70.

Wolfe AP and Siver PA. 2009. Three extant genera of freshwater thalassiosiroid diatoms from middle Eocene sediments in northern Canada. American Journal of Botany 96(2): 487-97.

Yang X, Anderson N, Dong X, Shen J. 2008. Surface sediment diatom assemblages and epilimnetic total phosphorus in large, shallow lakes of the Yangtze floodplain: Their relationships and implications for assessing long-term eutrophication. Freshwater Biology 53(7): 1273-90.

Chapter 2: Examining valve shape variation in *Eunotia* using geometric morphometrics

I**ntroduction:** As microscopic, photosynthetic eukaryotes, diatoms contribute markedly to primary productivity within aquatic environments (Dugdale and Goering, 1967; Falkowski et al., 1998). Diatoms are abundant and diverse as phytoplankton and benthic organisms. Globally, diatom species diversity is estimated to be upwards of 100,000 species (Mann and Vanormelingen, 2013). Though diatoms persist in a variety of habitats, individual species have been shown to correlate with certain water conditions (e.g., pH, nutrient levels) and have specific habitat preferences, thus serving as environmental indicators (Mangadze et al., 2016). The siliceous remains of diatoms are not degraded easily; thus, diatom walls can persist in sediments for long periods of time. Paleolimnologists use such sediments and knowledge of species' environmental preferences to reconstruct past environmental conditions (Katrantsiotis et al., 2016).

Diatom cells form a siliceous wall known as the frustule. The diatom frustule is formed from three siliceous components, the epivalve, hypovalve and one or more cingulae. The epivalve sits above and rests slightly over the hypovalve, and these two components are connected by cingula, which are open bands also referred to as girdle bands. Although the valves limit growth in one plane, additional girdle bands can be added, effectively spreading apart the valves and allowing for growth in frustules width. Structures such as pores, and/or areolae, may be present along the valve face, allowing the diatom to interact with the extracellular environment. Although often used interchangeably, fine distinctions exist between areolae and pores, mainly concerning the level, or depth, at which they occur within the silica of the valve wall. At their simplest, areolae represent occluded openings through the basal,

innermost siliceous layer of the valve whereas un-occluded areolae are often deemed pores (Ross et al., 1979). Areolae and/or pores arranged in a banding pattern akin to linear striations are referred to as striae (Round et al., 1990).

Diatoms exhibit a vast array of cell shapes and ornamentations, however it has long been convention to separate diatoms into two broadly defined groups, namely the centrics and pennates. Centric diatoms possess radial symmetry in valve view, whereas pennate diatoms may possess bilateral symmetry, or be asymmetrical about the apical axis and/or transapical axis (Round et al., 1990). The pennates are further subdivided into the raphid and araphid pennates, where, in the former, the raphe is a slit within in the cell wall used in movement (Ross et al., 1979; Round et al., 1990). Traditionally, the shape and ornamentation of the silica walls is used to delineate not only species but also taxonomic levels up to, and including, classes of diatoms. As such, morphology of the silica wall is the basis for diatom taxonomy (Patrick and Reimer, 1966). Scientists follow the morphologically based taxonomic scheme of Round et al. (1990) despite anticipated taxonomical revisions given the increasing prevalence of molecular systematics. However, given the overwhelmingly large number of diatom species and limited availability of sequence data for the majority of diatom species, the widespread implementation of DNA sequence data in diatom taxonomy and systematics has been slow (Theriot et al., 2011).

Despite being the dominant approach, the use of morphology can be challenging and even misleading in diatom taxonomy. One factor in this challenge is the cell cycle of diatoms, which has been understood for quite some time (Geitler, 1932). When diatoms reproduce asexually through mitosis, the parental hypotheca and epitheca separate to form daughter cells, each becoming the epithecum of the new cell. As a result, one daughter cell retains the original size of the previous generation, whereas the sister cell becomes slightly smaller in diameter. The

resulting successive reduction in frustule size has marked effects on valve features (Mann, 2011). For a given diatom species, a range of cell sizes can be observed within a population, especially given the effects of multiple rounds of cell division. This phenomenon of cell size reduction through successive rounds of cell division is known as the MacDonald-Pfitzer rule, which states that there is a gradual decrease in mean cell diameter with increasing population size (Laney et al., 2012). Phenotypic plasticity and environmentally induced teratological forms also may result in changes of overall cell size and morphology, further challenging morphological-based species identification (Cox 2014). Therefore, in diatom taxonomy, it is imperative to account for the changes in shape that accompany decreases in size due to cell division.

Diatoms are an evolutionarily young group of algae, originating no earlier than 240 Ma according to molecular estimates, with fossil records dating them to 180 Ma (Medlin and Kaczmarska, 2004). The first diatoms were centric diatoms and occurred in marine habitats; they colonized freshwater habitats later, with most molecular estimates dating the freshwater transition to the Cenozoic (c. 66-16Ma), with fossils dating the events to 50-45Ma (Sims et al., 2006). Recently there has been an interest in investigating morphological evolution of major groups of diatoms, with comparisons of extant and fossil taxa. For example, Lazarus et al. (2014) examined morphological disparity of diatoms and noted that diversification has been correlated to climactic changes during the Cenozoic. Following a rapid expansion of morphospace within the Cenozoic in major diatom groups, marine diatom morphospace has been largely static (Kotrc and Knoll, 2015). However, since the Eocene-Oligocene boundary there has been an increase in complexity for marine centric diatoms (Pappas, 2016). Other studies focusing on the Eocene have addressed the taxonomy of resting spores of marine pennate fossil taxa (Suto et al., 2009). Few studies have focused on the evolution of freshwater diatoms over geological time.

An important locality for freshwater fossil diatoms and other taxa is the Giraffe locality located close to the Arctic Circle in Canada. The Giraffe Pipe (GP) sediment core features the remains of a middle Eocene Maar Lake, formed during emplacement of a kimberlite, that persisted for approximately 7-8 million years before becoming terrestrialized and much later entombed with glacial till (Siver and Wolfe, 2009). Originally drilled as a prospect for mining diamonds, the core features exquisite preservation of siliceous remains, including freshwater sponge spicules, chrysophyte cysts and scales, and diatoms. All told, the GP core is 163 m in length, with a total of over 70 m of lake sediments after correcting for the dip of the core (Siver et al., 2013). The maximum age for the lake sediments was determined to be 47.8 ± 1.4 Ma by a $^{87}Rb/^{87}Sr$ model from kimberlitic phlogopite. Tephra layers that occur at the transition from lake to marsh sediments, representing complete backfilling of the lake, date to 40 Ma (Wolfe et al., 2006; Siver and Wolfe, 2009 and references therein). The Giraffe Pipe is unique in that it features some of the oldest remains of freshwater pennate diatoms. This record suggests that raphid pennate genera such as *Actinella* and *Eunotia* have persisted since at least the Eocene (Siver et al., 2015).

Eunotia C.G. Ehrenberg 1837 occurs in freshwater systems as both periphytic and planktonic species. The genus is near cosmopolitan in its distribution, oftentimes favoring humic, acidic and eutrophic conditions, though some forms have been noted to favor slightly alkaline, oligotrophic waters as well (Siver and Hamilton, 2011). Over 500 species of *Eunotia* have been described (Kulikovskiy et al., 2015). Characterized by a "strong back" and semi-lunate valve (Figure 1), *Eunotia* can exhibit a wide variety of morphological variation, most notably along the dorsal margin of the valve. Valve morphology ranges between those of great length and no apparent curvature to specimens with slight undulations upon the dorsal margins; in the most

extreme cases, numerous distinct “humps” abound along the dorsal margins (Patrick and Reimer, 1966). The GP specimens indicate that non-marine *Eunotia* now extend back into the Middle Eocene (Siver & Wolfe, 2007; Siver et al., 2015).

Geometric morphometrics allows the comparison of shapes defined by “landmarks” that are placed either directly upon, or in close association with, structures of biological relevance (Bookstein, 1997). Landmark analysis can also include non-permanent, or “sliding”, landmarks. This tool allows us to investigate shape independently from the influence of size. Sliding landmarks can aid in removing biases, through General Procrustes Alignment and centroid determination (Adams et al., 2004), introduced by the scientist, adding further resolving power to the analysis of biological structures. Morphometrics has been used previously in the study of diatoms (e.g., Stoermer and Ladewski, 1982) with specific applications to species-level systematics detailing species boundaries among morphospecies (Fránková et al., 2009), and in broad scale studies of shape evolution across all diatoms (e.g., Kotrc and Knoll, 2015). Given the extensive fossil record of diatoms preserved in marine and freshwater sediments, morphometrics allows us to compare morphological shape variation within fossil and extant taxa.

In this study, I will conduct a genus-level investigation of evolution for the pennate freshwater genus *Eunotia* using landmark analysis. This study will compare an extensive dataset of modern specimens with fossil specimens taken from multiple strata from the Giraffe core. Each stratum represents a distinct snapshot of geologic time during the Middle Eocene. I will investigate the evolution of morphology, and concomitant change in morphospace, from the Eocene to the present, examining disparity and the assumptions of increasing morphological variance over time. As the taxonomical assignment of fossil *Eunotia* is incomplete, we cannot use species richness as a metric for investigating *Eunotia* evolution. Instead, I will compare the

shape of *Eunotia* specimens within a common morphospace. The benefit of this approach is that it allows for comparisons between fossil specimens and extant taxa, regardless of unclear or incomplete taxonomical assignment. The assumption that changes in the shape of *Eunotia* represent expansions into different habitats or niches allows us to infer how *Eunotia* may have evolved since this time period.

Methods:

Specimen Acquisition: An initial dataset from Bishop-Genovesi (2014) referenced scanned monograph plates from Patrick and Reimer (1966) and featured 66 specimens representing 60 species. It also used information from and Siver and Hamilton (2011), which contained 43 specimens representing 23 species. These references were restricted to temperate, North American diatom taxa. In the present study, my goals were to expand this dataset by adding specimens representing tropical and South American taxa and to enhance the sampling of fossil specimens. The aforementioned method of scanned monographic plates was applied to the current study with 157 tropical specimens (69 species) from South America and Florida, U.S.A, from Metzeltin and Lange-Bertalot (1998). Additionally, type material representing 13 species was accessed from The Diatom Herbarium at the Academy of Natural Sciences at Drexel University. New sampling also featured non-type material, especially from tropical locations, for a total of 97 specimens. Both online holdings as well as original images taken from prepared slides were used. In all, 632 specimens representing 133 extant species and 248 fossil specimens were included. Where available, extant specimens were imaged in multiples of three in an effort to capture upper and lower bounds of valve shape over a known size range. Some specimens lacked associated taxonomic data, including all fossil specimens and materials from the Academy that could not be identified to species. In these cases, each fossil specimen has a

unique number (e.g. Eunotia_120) whereas those from the Academy are numbered according their slide of origin within the Academy's General Collection (e.g. "GC26658_8" is the 8th specimen from slide GC26658) (see Results, Appendix 1). For fossil material, absolute dates for the core samples are not known; therefore I am using core depth as a proxy for age with the deepest sections of the core being the oldest.

Image Acquisition: Images of fossil *Eunotia* from the Giraffe Pipe core were taken using an Olympus BX51 microscope using a Sony DKC-ST5 camera interfacing with a Dell Precision T1600 computer running Windows XP Professional Edition 5.1. All images were taken at the Freshwater Ecology Lab at Connecticut College. Original images of extant specimens also were acquired from material within the General Collection at The Diatom Herbarium at the Academy of Natural Sciences of Philadelphia at Drexel University and were used alongside the aforementioned monographic plates.

Orientation: All images were standardized to 300dpi and cropped in ImageJ software (freely available from http://imagej.nih.gov/ij/index.html) (Rasband, 2015). Bishop-Genovesi (2014) used a similar procedure, although he standardized images in Adobe Photoshop 4.0.1. As a final step, all images were oriented with the dorsal margin facing the left portion of the screen, with a vertical axis of 90 degrees. All specimens used in the analysis were in valve view.

Measures: In ImageJ (Rasband, 2015), measures of valve characters were taken, and guidelines were placed on the specimens for digitization. This step ensured that permanent landmarks were placed accurately upon each specimen (see Guidelines). Total length of the valve was measured from the proximal to distal apex using points that featured the greatest extent in length. The width of the valve was determined at the midpoint of the length measurement. Total length of the dorsal and the ventral valve margins were determined using guidelines in the trace function of

ImageJ, beginning with the distal portion of the valve and ending at the opposing, proximal apex.

Striae Density: Striae density per 10 μm was recorded along the midline of the valve (Patrick and Reimer, 1966; Siver and Hamilton, 2011). Along the midline of the valve, where the width measurement was taken, a 10 μm line segment was superimposed upon the image on top of the width measurement, so that segment was in the exact middle of the width measurement with 5 μm extending in each direction from the width line. Only those striae that contacted the line segment were counted. The way in which striae are measured can vary (see discussion).

Guidelines: A total of four guidelines were put on the image to aid in the placement of permanent landmarks for morphometrics analysis. Two were established using the valve width measurement, wherein a straight line was laid across the valve face. Determining the width of each valve apex created the last two guidelines for digitization. For each apex, between two to four separate measurements were taken, becoming progressively smaller. From the midpoint of these measures, a line was drawn extending through the valve apex. Here, this line determined the boundary between the dorsal and ventral valve margins.

Digitization: Geometric morphometric data were collected for all specimens using Tps-series software (Rohlf 2007). Images were first compiled in a .TPS file using TPSUtil. Landmark superimposition was performed in TPSDig2. A slider file describing the relationships between landmarks was created in TPSUtil. These files are available in Appendices 2 and 3 (see results). This software is freely available from the Stony Brook University Morphometrics page (http://life.bio.sunysb.edu/morph/). A total of 80 landmarks were used in the analysis (Figure 2). Of these, 76 semi-permanent landmarks, also known as sliding landmarks, were placed along the valve margin between the 4 permanent landmarks. Proximal and distal valve apices in valve view of the frustule represented two permanent landmarks, 1 and 47, respectively. Two

additional permanent landmarks were placed along the midpoint of the valve, along their respective dorsal and ventral margins, corresponding to landmarks 24 and 67. The midpoint of the valve was determined using both length and width measurements to accurately place landmarks 24 and 67.

Data Analysis: General Procrustes Analysis (GPA), alongside other morphometrics analyses, was carried out in R (freely available from https://cran.r-project.org) using the "geomorph" package (Adams and Otarole-Castillo, 2013). GPA scores were then used within a principal components analysis. The PCA scores were exported and saved, alongside added ecological data, and then plotted in R. All PCA graphs are based on the coordinates first generated in the GPA. Disparity measures were also calculated using the "geomorph" package based upon pairwise distance comparisons initially computed during the GPA. A one-way analysis of variance (ANOVA) using pairwise distances was performed comparing the mean, or centroid, against all specimens in the study (n=632).

Results:

A total of 632 specimens were included in the analysis, 384 of which represented extant taxa and 248 of which were from fossils (Appendix 1). Extant specimens comprise over 100 species, varieties and forms of *Eunotia*. A total of 97 specimens, including types, were imaged from prepared slides in the Diatom Herbarium General Collection at The Diatom Herbarium at the Academy of Natural Sciences of Philadelphia at Drexel University. Appendix 1 can be found online through Digital Commons at the University of Connecticut (http://digitalcommons.uconn.edu), where is it attached to this thesis as a supplement within "Additional Files". Original images have been deposited online within the Morphobank database (www.morphobank.org) as Project number 2518. A summary of known species and their sources

is seen in Table 1. A total of 248 fossil specimens originating from the Giraffe Pipe sediments were imaged from prepared slides. Table 2 displays information for fossil specimens, including the origin of the sample, referred to by box number, alongside the corrected depth in the core and estimated depth in the lake proper. A file containing the landmark data that was analyzed in TPS and the slider file can be found in Appendix 2 and Appendix 3.

I report analyses from all specimens first, followed by analyses that divide the specimens by time (fossil v. extant), habitat (temperate v. tropical, for extant), geography (extant specimens only), depth within the GP core (fossil specimens only) and location within the water column (benthic v. planktonic, extant specimens only). Trends were investigated through ordination along principal components axes, and statistical significance of trends were determined using one-way analysis of variance (ANOVA) for linear measures taken from the specimens. Lastly, pairwise distances are utilized in testing the amount of morphological change, or disparity, between subsets of data.

The results of a principal components analysis (PCA) for all specimens are shown in Figure 3. This graph was generated after a general Procrustes alignment (GPA), which computes the average Procrustes distances for each landmark (n=80) for each specimen (n=632). Located at the origin of the plot, the centroid, or mean, represents the average Procrustes distance for all specimens for all landmarks. Displayed at the extremes of the first principal components axis are thin spline diagrams, showing the change in shape that is accounted for when progressing along the first axis. Overall, there is maintenance of overall concavity of the valve. Generally, more ornamented dorsal margins are associated with valves at the lower range of total valve length.

The morphospace occupied by *Eunotia* is quite varied (Figure 4). The first principal components axis (x-axis in Figures 3-4) displays changes in the overall shape of the valve from

positive to negative, namely a gradual increase in width-to-length ratio. This occurs alongside a concomitant change in convexity of the dorsal margin. There is a slight change in dorsal margin swelling as the outer bounds of the first principal components axis are approached on the negative side. So, too, we see a smaller length to width ratio and larger dorsal length to ventral length ratio (Figure 4). Opposing these are slender valves with a gentler concavity. These are longer in overall length, quite slender in width, and approaching the positive end of the first principal components axis. These valves show few ornaments about either dorsal or ventral margins, and instead show more pronounced valve apices. Along the second principal components axis (y-axis) we see constrained valve apices and significant variation in concavity, with flatter valves at the positive end of the axis and concave values at the negative end. Dorsal ornamentation is also accounted for in the second axis, with two distinct dorsal undulations, or humps, giving valves at the negative end an apparent transapical symmetry, giving way to a reduced, centralized undulation at the positive end. Length is relatively conserved, as this axis is responsible for the addition of simultaneous changes in width and dorsal ornamentation.

Approximately 95% of cumulative shape variance is explained by the first 10 axes of the PCA, with the primary axis accounting for over 72% of the overall variance (Table 3). Recall, a total of 80 landmarks were used in the analysis, setting the upper bounds of axes used within the PCA. As such, axes along principal components demonstrate relationships graphically along in a number of dimensions equal to the number of landmarks in the analysis. Although it is most common to project the PCA in two dimensions (Figure 3), displaying relationships in three dimensions (Figure 5) can help visualize the degree to which morphospace around the centroid is occupied, and the amount of morphospace occupied in total. In three dimensions (Figure 5)

Eunotia morphospace expands in all directions from the centroid, but, by definition, variance decreases on higher-numbered axes..

Following the initial PCA, the data set was subdivided in order to investigate relationships between morphospace and a number of variables classifying the taxa. My goal was to determine if there are relationships among these variables and occupied morphospace. The largest data subsets investigated modern and fossil specimens. From these, additional subsets were examined: taxa were grouped by climate, allometric trends were briefly examined for two taxa, geographical origins, position within the water column for extant specimens and, for fossil specimens, depth within the GP core.

A simple comparison of extant (Red, n=384) and fossil (Black, n=248) specimens illustrates that morphospace occupation is greater in the extant specimens than the fossil ones in all directions (Figure 6). Recall, the fossil specimens from the Eocene Giraffe Pipe core represent the oldest known specimens of *Eunotia* and thus represent the oldest known morphologies for the genus. Interestingly, both modern and fossil specimens greatly overlap in the shape space around the centroid, here at the origin of the plot. Again, this centroid is the "mean" shape of *Eunotia* calculated for all landmarks (n=80) for all specimens (n=632) within the analysis. In general, fossil specimens are more restricted and comprise a subset of the morphospace occupied by modern taxa, which occupy and expand upon the morphospace exhibited in the fossil specimens.

Dividing the extant taxa by climate, we see a large co-occurrence within the morphospace of the temperate (Black, N=152) and tropical taxa (Red, N=232) (Figure 7), with fossil specimens (Grey, N=248) largely clustered around the origin of the plot, representing the centroid of the analysis. There is an expansion of the tropical taxa towards the extremes of the PCA axes; namely towards the boundaries responsible for modifications at the dorsal margin and

valve apices (Figure 7). On the right hand side of the graph, we see that members of both habitats occupy a similar, tightly clustered cloud within the morphospace whereas on the left side of the plot, we see the tropical taxa occupying a larger swath of the morphospace, with brief punctuations of temperate taxa, that directly contrasts the restricted morphospace of the right side of the graph.

Trends in allometry for two species show different trajectories (Figure 8), highlighting the importance of sampling multiple specimens of the same taxon in order to capture the size series. Here, multiple specimens of *Eunotia ventriosa* (Red, N=10) and *E. arcuoides* (Blue, N=10) are highlighted. All specimens from *E. arcuoides* were photographed from type materials, including the type series and from multiple individuals from the type locality. The fine clustering of morphospace for this species is noteworthy when compared to the morphospace occupied by *E. ventriosa*. When the centroid sizes for both *E. ventriosa* and *E. arcuoides* are compared to the results of the first principal components analysis, we see that *E. ventriosa* centroid sizes expand from the negative to positive ends of the first principal components axis (Figure 9), suggesting that shape change is seen within allometric growth, whereas within *E. arcuoides* this may be present but to a lesser extent, or rather, that the resultant shape change is less apparent on the first principal components axis. Specimens of *E. ventriosa* were sampled from two geographic locations, including the type locality. Specimens of *E. ventriosa, E. ventriosa* variety *brevis* and *E. brevis* were lumped together when first described, as in this analysis, though the taxonomic standing for this species complex currently separates them as in Metzeltin and Lange-Bertalot (1998).

Comparing centroid sizes against the scores of the first principle components axis, we see evidence of among-species allometry in *Eunotia* (Figure 10). Small- and medium-sized

specimens vary widely in PC1, although the smallest specimens do no show the most positive values. In contrast, large specimens all plot at the positive end of the axis. In other words, large specimens are always long and skinny. Modern specimens have a larger spread, whereas the fossils are more tightly clustered and more limited in their centroid sizes (Figure 10). Modern specimens possess a larger spread as well when comparing centroid sizes and PC2 (Figure 11), which describes the convexity and dorsal ornamentation of *Eunotia*. PC2 is not correlated with centroid size, although small specimens are more variable on the axis.

This study focused primarily upon North and South American taxa, but still featured specimens originating from Africa and Europe, speaking to the cosmopolitan nature of *Eunotia* (Figure 12). We see limited occupation of morphospace by European and African specimens (red and yellow points), but this is due to limited sampling (22 samples; Appendix 1). However, specimens from the Americas span the entirety of the graph. Both North and South American taxa occupy a rather tightly constrained region of morphospace at the positive end of the x-axis that then blossoms into a large area at the negative end. This trend is more striking when European and African taxa are eliminated (Figure 13) where North American and South American taxa are compared against one another, in black and red, respectively. The distinctions between North and South American taxa and between taxa from temperate and tropical climates are slightly different, though appearing quite similar, and this is due to the large number of specimens from Florida, U.S.A, which are classified as tropical but occur within the contiguous United States.

The shapes of fossil specimens from six different depths in the GP core, representing approximately seven million years of sediments, vary among samples (Figure 14), suggesting that taxonomic composition may be dependent on the lake (successional) conditions, which

varied through the Eocene. Most notably, the specimens from the lowest three samples (yellow, black, and orange) all plot in a restricted region of morphospace, whereas the upper three samples (blue, light blue, and red) occupy this region as well as well as an additional region.

Modern tropical taxa were compared against fossil tropical taxa (red and orange symbols, respectively, in Figure 15) with temperate specimens indicated in white. Fossil tropical taxa are still quite constrained in morphospace; modern specimens occupy and extend the morphospace occupied by the tropical fossil specimens. Of particular note, morphospace around the centroid is highly populated with fossil specimens, but the fossils do not occupy as wide a range as the modern specimens. Towards the left side of the graph, forms of *Eunotia* become more ornamented about the dorsal margin and more stout, suggesting that there was an expansion into morphospace occupation corresponding to these forms.

To test for correlations between characters, linear regressions were performed using both raw and transformed (Log_{10}) data taken for all specimens (N=632) in Table 4. Results of the first four principal components axes were regressed against linear measurements. Linear regressions were also performed on subsets of the data in order to investigate the possible biases introduced in the data and directionality of results. Linear regressions of extant temperate (Table 5), extant tropical (Table 6), fossil (Table 7) and finally total extant taxa (Table 8)**,** comprising both temperate and tropical extant specimens were performed. In general, the primary 3 axes yielded significant relationships, while the fourth PCA axis most often did not. Of the 3 axes, the primary and secondary PCA axes features the strongest correlations, respectively. Seeing these relationships, we know that the primary axes of the PCA account for the variety of shape changes occurring along the valve. Historically for *Eunotia*, ordination along principal

components follows a generalized scheme, with each axis correlated to a particular change in shape, or character, of the valve (see discussion).

Results of a one-way analysis of variance are displayed in Table 9. The first two principal components axes were compared against the dataset divided to examine relationships between age, climate, continent of origin and fossil depths. Post-hoc analysis was done with Tukeys comparison of multiple means, here reported at the 95% confidence interval. Results demonstrate significance between the primary and secondary PCA axes and the subsets of data divided by age and climate, though stronger relationships are seen within the primary (first) PCA axis. These same results were not seen for the smaller subsets of data, particularly the subset of fossil depth and continent data (those with smaller mean sample sizes). First, data were compared using their continent of origin, then a smaller subset examining only those specimens originating within the Americas, and finally fossil specimens were examined by their corresponding depth within the GP core. The continent and Americas subsets were significant for the secondary, not the primary axis. Fossil specimens separated by depth showed the significance about only the primary axis of the PCA. However, given the small mean of particular samples within the fossil dataset, we suggest this result may appear significant in large part due to larger sample size for particular GP sections.

Disparity was measured through aligned Procrustes pairwise distances. Distances were calculated by performing a general Procrustes alignment (GPA). This alignment was performed on each of the 74 sliding landmarks for all specimens (N=632). While the GPA is the first step within geometrics morphometrics landmark analysis for shape, pairwise distances provided a statistically valid means for comparison of shape evolution through one-way analysis of variance (Adams and Otarola-Castillo, 2013 & references therein). The first comparison, a one-way

analysis of variance (ANOVA) using pairwise distances, compares the mean, or centroid of the dataset, calculated from using the alignment data for 74 sliding landmarks, for each of these landmarks, for every specimen against the dataset as a whole. From these pairwise distances, it was shown that the centroid, or mean specimen, differs significantly from the remainder of the dataset (Table 10). Specimens differing greatly from the mean will appear further away (when displayed along principal components) from the centroid than those specimens varying to a lesser extent. Additionally, this suggests that the dataset contains specimens for which Procrustes distances vary significantly from the mean; large distances of movement suggest larger variances in shape.

To investigate the cause of this significance, we used pairwise distances to investigate differences in shape between subsets of the data. We see a significant difference among the fossil specimens and extant taxa, suggesting an increase in morphological change (Table 11). Modern specimens as a whole show a larger Procrustes variance than fossil specimens. Analysis for disparity was also performed to examine possible relationships between morphological change and climate. Also worthy of note, we see this same trend analyzing the subset of data for extant temperate and extant tropical taxa alongside fossil taxa (Table 12). Tropical taxa show the largest Procrustes variances, followed closely behind by temperate taxa. Fossil specimens demonstrate the lowest variance in Procrustes distances; again suggesting their shape is relatively constant. When comparing differences between extant tropical taxa and fossil specimens, we see a significant result in the absolute pairwise distances between the groups. A significant result is also seen when fossil specimens are compared to extant temperate taxa, though the pairwise distances suggest that the tropical are more different than the temperate taxa when compared against fossil specimens. We also see that extant tropical and extant temperate taxa do not differ

when compared via pairwise distances (Table 12). Finally, both extant tropical and temperate taxa were compared against the GP core sections. Though small sample sizes can have an effect on these measures, we do see significant results between the heavily sampled sections of the GP core (Boxes 13 and 15-1-131) and extant tropical taxa (Table 13). We do not see significant differences between GP samples; however, we do see differences in pairwise distances. Though the pairwise comparisons are not significantly different between sections, these data are still useful in demonstrating that the core does not appear to display a homogenous morphology across section (time). Overall, these results suggest that there has been morphological change in tropical taxa across a temporal gradient.

Comments on "periphytic/planktonic" morphospace: Thin spline diagrams (Figure 4) demonstrate particular trends within the morphospace. If we compare particular specimens, and their resultant measures, we may be able to glean insight into particular morphospace of taxa, as it pertains to *Eunotia* taxa being planktonic or periphytic. Appendix 1 compiles known data for all specimens within the analysis. It is noted that some specimens lack information about where in the water column the collection was made. Only records with explicit collection data stating where within the water column the specimen was collected were used for this analysis. Generally, planktonic taxa are expected to be much longer than they are wide, with a resultantly large length: width ratio. Qualitatively, we see them as pencil-like, with reduced raphes. We would also expect the dorsal length to ventral length ratio to be around 1 as well, suggesting a lack of ornamentation about the valve margins. Conversely, epiphytic taxa are expected to possess a relatively smaller length to width ratio, being stouter overall. Valve ornaments may vary, but a characteristic concavity is pervasive. Raphes may be quite distinct. Although data are limited, we see that both planktonic and epiphytic forms occupy similarly wide portions of the

morphospace (Figure 16). These results are surprising because planktonic and epiphytic specimens overlap greatly, and it appears that there is no relationship of shape to the distribution in the water column (planktonic or epiphytic).

Discussion:

The goal of this study was to characterize the shape changes exhibited by *Eunotia* when comparing its oldest known representatives with an extensive extant taxa dataset. We compare fossil and extant taxa in order to investigate the expansion of morphospace in the genus. Applied more broadly, we are investigating morphological evolution, which has been explored in macroscopic taxa (Foote 1993) but with limited exploration within the diatoms, especially those lacking molecular sequence data. Inherent in this comparison is the comparison of shape change across ecological boundaries. However, if we are to truly capture the shape changes exhibited in *Eunotia* from the middle Eocene to present, we must carefully control for ecology and compare *Eunotia* from similar habitats.

Realizing the limitations within Bishop-Genovesi (2014), which relied on smaller numbers of both fossil and extant specimens and an emphasis on temperate extant taxa, the present study set out to expand upon the aforementioned dataset. Bishop-Genovesi (2014) featured samples from two sections of the GP core and modern taxonomical references from temperate climates (Patrick & Reimer, 1966; Siver and Hamilton, 2011) and demonstrated significant differences between modern and fossil specimens of *Eunotia*. However these findings were limited, as there was no correction for the climate of the Giraffe Pipe lake environment and extant samples featured only North American taxa. The Giraffe Pipe sediments were determined to represent the remains of a tropical lake (Pisera et al., 2013; Siver and Wolfe, 2009) so the

fossil specimens should be compared to modern specimens from an analogous, tropical climate. The study at present has expanded fossil sampling, adding specimens from 4 additional sections of the core (Figure 14) to more accurately describe the morphospace occupied by *Eunotia* within the middle Eocene when it was first seen within the non-marine habitat. Additional modern taxa have been added as well, with a focus towards adding taxa from tropical climates. In this case, these were from the South American continent, with a few specimens present from Africa (Ghana). Concerning the addition of modern taxa, efforts were made to add specimens within a species' size series to capture the range of morphospace occupied by members of the same species population. In this respect, we aimed to capture the breadth of morphology of *Eunotia*. Using the extant tropical taxa, we can now compare extant and fossil taxa from similar habitat regimes. Additionally, with added fossil sampling and extant temperate taxa, we can compare extant taxa to examine shape variance, and use the dataset as a whole to examine the temporal change in morphospace as a whole. These divisions within the dataset allow us to correct the data for climate and geography. As such, I sought to quantify the differences between specimens first by examining the morphospace occupied by them when displayed along principal components. Secondly, I sought to examine relationships between subsets of data when compared against the principal components axes and to test for significance via ANOVA. I sought to quantify the morphological shape change, or disparity, between subsets. In all these analyses, I first compared the broadest data subsets, distinguishing fossil and extant taxa. Next, subsets of data were compared based upon geography, to determine if there was a geographical influence within the data. Lastly, we examined the climactic components; namely those between extant and fossil tropical taxa. Results show that these subsets of data are each unique, and also differ from one another. Most strikingly, results shows that tropical taxa compared across a

geological timeframe have changed since the Eocene. In particular, we see that tropical extant taxa occupy a larger array of morphological states. They are much more varied, and more finely ornamented than fossil specimens, one caveat being that extant specimens were collected from a number of different localities whereas fossil specimens represent a single locality. Our study is unique in its approach, as it was chiefly concerned with the morphospace occupied with the entirety of *Eunotia*, as opposed to individual taxa within the clade.

Generally, diatoms studies utilizing morphometrics can be classified as either shape analyses, which use differences in shape to evaluate biological hypotheses, or pattern recognition, which is used for binning specimens with the goal of determining species or other taxonomic categories (Pappas et al., 2014). In this study, our goal was to characterize the overall morphospace of *Eunotia* and to describe the trends in the morphological evolution of the genus. As such, our methods have focused on characterizing the shape change within a genus of diatoms, as opposed to the shape change within a particular species. Secondly, our study differs again, as we do not seek to bin our specimens into particular taxonomic categories, or species. Multiple specimens of the same species were included because of their variance in morphology. This study does not seek to confirm existing taxonomy, nor to disprove existing species concepts attached to them. Standard geometric morphometrics has mainly been used to examine shape change at the species or subspecies level (e.g., English and Potapova, 2012), so the present study is unique in addressing variation at the genus level.

Kotrc and Knoll (2015) discussed trends in the evolution of morphology in Cenozoic planktonic marine diatoms. Their study identified specimens to the level of genus but did not investigate each genus separately. Rather, pooled data described overall temporal trends. Their interpretation of expanding morphospace since the Cenozoic is due, they suggest, to sampling

biases within the *Neptune* database. In part due to geological preservation, more recent deposits introduced larger taxon datasets. This was apparent too, with their self-culling of data, based upon the morphological characters they chose for their data matrix. Kotrc and Knoll (2015) argue that the disparity measures (as mean pairwise distances and alpha volume per genus) point to a stasis of morphospace. Pairwise distances were used to discuss the differences between taxa, whilst alpha volume was used to discuss the amount of morphospace occupied as a whole. However, their study was focused upon marine planktonic taxa. Our findings utilizing pairwise distances suggest an expansion of morphospace since the Eocene, with regards to a freshwater pennate genus. This further supports previous work suggesting pennate diatoms were well established in the Eocene (Siver et al., 2010). However, it is difficult to determine if this expansion of morphospace is linked with a subsequent expansion of niches. As previously mentioned, Kotrc and Knoll (2015) carefully defined their morphological characters within their data matrix. They brought careful attention to standardization of methods, and omitted specimens when needed. The standardization of features upon the valve face presented in Kotrc and Knoll (2015) was continued within this study, with attention being paid to striae, especially.

Measuring striae density is a convention among diatomists, though because striations may differ across the valve, it is commonplace to indicate from where on the valve the measures are taken (Patrick& Reimer, 1966). This measure does not take into account variability of striae density across the entirety of the valve face. For example, striae density, here taken at the midpoint of the valve, has been observed to increase or decrease in density as the valve apices are approached. Additionally, this measure assumes linearly placed striations across the valve, from dorsal to ventral margin. While not typical in *Eunotia*, species such as *E. punctastriata* exhibit a single striation arranged along the dorsal margin. *Eunotia reimeri* features prominent

hyaline areas and a scattered pore field, as opposed to the common linear striations, across the valve. Factors that could contribute to a lowered striae density include: Specimens not possessing linear striae, or their pore organization differed from those linearly displayed across the valve. Additionally, fossil specimens may display varying levels of striae preservation, even across a single specimen. Given the variability displayed within this morphological characteristic, it was our goal to standardize the measurement for the overwhelming majority of the specimens examined within the study.

These results demonstrate consistency with respect to PC axes previously summarized for *Eunotia*. Although limited, early works described trends among *E. pectinalis* displayed along principal components axes (Steinman and Ladewski, 1987; Pappas et al., 2014). Though the present study is markedly larger in the number of taxa represented, it is an interesting parallel that the results from those studies of *E. pectinalis* display similarities with regard to the axes of the principal components analysis. It is worthwhile to note that the present study contains specimens of *E. pectinalis* as well, described from a number of locations within North America (Appendix 1). However, it is important to note that comparisons made between the early morphometrics literature and the current study should account not only for the scope, but also for the morphometrics methods used, as there are a number of approaches. Here, we used landmark based geometric morphometrics whereas discriminant analysis (Steinman and Sheath, 1984) and Legendre polynomials (Steinman and Ladewski, 1987) were used previously, though the latter study did feature PCA and MANOVA generated from Legendre polynomials. Though outside the scope of discussion within the present study, methods featuring Legendre polynomials may still be utilized within particular investigations (Adams et al., 2004; 2013). In their shape analysis of *E. pectinalis*, Steinman and Ladewski (1987) saw the concavity of the valve develop

along PC3. Furthermore, extending the analysis to the 6th or 7th axes may better characterize the shape changes seen within *E. pectinalis,* corresponding to increased apex size and ventral inflation, respectively (Pappas et al., 2014). However, in the present study, PC2 shows the development of valve concavity for *Eunotia* specimens, alongside concomitant changes to valve apices In the present study, given the variance displayed by the primary two axes, and their attributed cumulative change (Table 3), we suggest that the trends of PCA axes seen in Steinman and Ladewski (1987) and summarized in Pappas et al., (2014) are a result of the methods applied to their respective studies which sought to quantify the shape change within a single taxon, *E. pectinalis*, whereas in the present study, we sought to characterize the shape of the genus as a whole. However, the present study allows brief comparisons amongst individual taxa and suggestions for further work, as type material was compared against other specimens of a species within its range.

Allometric trends investigated within two *Eunotia* species, *E. ventriosa* and *E. arcuoides* (Figure 8 and Figure 9) demonstrate the utility of geometric morphometrics coupled with extensive sampling. It highlights that taxonomic boundaries of species can be explored with geometric morphometrics. Of particular note is the tightly clustered area of morphospace occupied by *E. arcuoides* due to the presence of multiple specimens from the type locality of the species, including the type specimen series. The restricted area of morphospace occupied by a number of specimens in close proximity to one another would suggest that these specimens belong to the same species. However, when a species occupies a larger area of morphospace, as seen with *E. veneroides*, the taxonomic decision to include the group into one species becomes more difficult. Here, we chose to group together the species complex of *E. veneroides* to demonstrate the difficulty of taxonomic decisions concerning the species, as it was first

described as a single species. This standing was later changed to include *E. veneroides* and a sub species, *E. veneroides var. brevis*; this latter variety folded a separate species (*E. brevis*) into the sub-species, *E. veneroides var. brevis* (Metzeltin and Lange-Bertalot, 1998). Though outside the scope of this study, this small-scale demonstration concerning the taxonomic history of one species suggests that alongside other data, such as habitat and ecological regimes, geometric morphometrics can be a useful aide in alpha taxonomy (English and Potapova, 2012).

Surprisingly, no relationship between shape and life style (planktonic or epiphytic) was observed for extant specimens of *Eunotia*. However, the present study relied upon the collection data associated with the monographs and thus, it was not possible to go collect this data personally. It was at times difficult to interpret where a diatom lived from where it was collected. Secondly, when these data were reported, detailed collection methods were most often not reported. In this way, it may be difficult to ascertain whether a particular species is planktonic, epiphytic, or, although not yet observed within *Eunotia,* exhibit a facultative switch between the "stages". What these results may demonstrate is that *Eunotia* may have a number of ways to achieve a planktonic existence, either as a solitary cell, or as a colonial form. Colonial forms have been observed in *Eunotia* (Wetzel et al., 2010). Interestingly, results do suggest a cutoff for ornamentation with regard to habitat and centroid size, as the largest cells along the positive extreme of PC1 (Figure 15) are seen to be those expected to be planktonic, i.e., large in length, low curvature and close to the positive axis of PC2 (Figure 15 and Figure 11).

Though the results of the present study are compelling, to more fully understand the evolution of shape change within *Eunotia* will require a well-resolved phylogeny for the genus. Currently, only a handful of DNA sequences of *Eunotia* are present in GenBank. Our results suggest that the genus may have expanded in morphospace occupation since the Eocene,

although Eocene forms are all within the range of morphospace occupied by extant forms, indicating that many frustrule shapes have persisted through time. However, without molecular data, it is difficult to estimate whether the observed changes happened gradually or through punctuated evolutionary events. Finally, additional tropical specimens from the African continent would allow a more complete understanding of the morphological distinctions amongst tropical *Eunotia*. This same idea expands to the polar regions as well.

In summary, this study expands upon previous findings of Bishop-Genovesi (2014) with regard to sample size, geographic coverage and robustness of methods, all of which are crucial in limiting potential biases within morphometrics studies (Pappas et al., 2014). Through ordination, one-way analysis of variance and measures of disparity, I demonstrate that there is great overlap in the valve morphology of *Eunotia* from the Eocene to present times, meaning that already at that point in time much of the variation that we see now was present. In addition, valve morphology in *Eunotia* has expanded since the Eocene, suggesting an expansion of available ecological niches. Lastly, I have demonstrated a significant difference in valve shape between tropical specimens from the Eocene and from the present day. This study expands the morphological diversity of diatoms being uncovered from the GP core (Siver et al., 2015) and demonstrates the utility of landmark based geometric morphometrics to investigate valve shape trends, and disparity at the genus level in diatoms.

References

Adams DC and Otarola-Castillo E. 2013. Geomorph: An R package for the collection and analysis of geometric morphometric shape data. Methods in Ecology and Evolution 4:393-99.

Adams DC, Rohlf FJ, Slice DE. 2013. A field comes of age: Geometric morphometrics in the 21st century. Hystrix, the Italian Journal of Mammalogy 24(1): 7-14.

Adams DC, Rohlf FJ, Slice DE. 2004. Geometric morphometrics; ten years of progress following the 'revolution'. Hystrix, the Italian Journal of Zoology 71: 5-16.

Bishop-Genovesi J. 2014. Evaluating trends in valve shape in *Eunotia* by comparing fossil and modern species. Undergraduate Thesis. New London: Connecticut College.

Bookstein FL. 1997. Landmark methods for forms without landmarks: Morphometrics of group differences in outline shape. Medical Image Analysis 1(3): 225-43.

Cox EJ. 2014. Diatom identification in the face of changing species concepts and evidence of phenotypic plasticity. Journal of Micropaleontology 33(2): 111-20.

Dugdale R and Goering J. 1967. Uptake of new and regenerated forms of nitrogen in primary productivity. Limnology and Oceanography 12(2): 196-206.

English JD and Potapova MG. 2012. Ontogenetic and interspecific valve shape variation in the Pinnatae group of the genus *Surirella* and the description of *S. lacrimula* sp. nov. Diatom Research 27(1): 9-27.

Falkowski PG, Barber RT, Smetacek VV. 1998. Biogeochemical controls and feedbacks on ocean primary production. Science 281(5374): 200-7.

Foote M. 1993. Contributions of individual taxa to overall morphological disparity. Paleobiology 19(04): 403-19.

Fránková M, Ková AP, Neustupa J, Pichrtová M, Marvan P. 2009. Geometric morphometrics-a sensitive method to distinguish diatom morphospecies: A case study on the sympatric populations of *Reimeria sinuata* and *Gomphonema tergestinum* (Bacillariophyceae) from the river Bečva, Czech Republic. Nova Hedwigia 88(1-2): 81-95.

Geitler L. 1932. Der Formweschel der pennaten Diatomeen (Kieselalgen). Arch. Prostistenk. 78: 1-226. Germany.

Katrantsiotis C, Norström E, Holmgren K, Risberg J, Skelton A. 2016. High-resolution environmental reconstruction in SW Peloponnese, Greece, covering the last c. 6000 years: Evidence from Agios Floros fen, Messenian plain. Holocene 26(2): 188-204.

Kotrc B and Knoll AH. 2015. A morphospace of planktonic marine diatoms. I. Two views of disparity through time. Paleobiology 41(01): 45-67.

Kulikovskiy M, Lange-Bertalot H, Witkowski A, Khursevich GK, Kociolek JP. 2015. New species of *Eunotia* (Bacillariophyta) from Lake Baikal with comments on morphology and biogeography of the genus. Phycologia 54(3): 248-60.

Laney SR, Olson RJ, Sosik HM. 2012. Diatoms favor their younger daughters. Limnology and Oceanography 57(5): 1572-8.

Lazarus D, Barron J, Renaudie J, Diver P, Türke A. 2014. Cenozoic planktonic marine diatom diversity and correlation to climate change. Public Library of Science One 9(1): e84857.

Mangadze T, Bere T, Mwedzi T. 2016. Choice of biota in stream assessment and monitoring programs in tropical streams: A comparison of diatoms, macroinvertebrates and fish. Ecological Indicators 63: 128-43.

Mann DG and Vanormelingen P. 2013. An inordinate fondness? The number, distributions, and origins of diatom species. Journal of Eukaryotic Microbiology 60(4): 414-20.

Medlin LK and Kaczmarska I. 2004. Evolution of the diatoms: V. morphological and cytological support for the major clades and a taxonomic revision. Phycologia 43(3): 245-70.

Metzeltin D and Lange-Bertalot H. 1998. Tropische Diatomeen in Südamerika, I. Koeltz Scientific Books. Iconographia Diatomologica 5: 695 p.

Pappas JL. 2016. Multivariate complexity analysis of 3D surface form and function of centric diatoms at the Eocene–Oligocene transition. Marine Micropaleontology 122: 67-86.

Pappas JL, Kociolek JP, Stoermer EF. 2014. Quantitative morphometric methods in diatom research. Nova Hedwigia, Beiheft 143: 281-306.

Patrick R and Reimer CW. 1966. The diatoms of the United States: Exclusive of Alaska and Hawaii. First ed. United States: Academy of Natural Sciences of Philadelphia. 688 p.

Pisera A, Siver PA, Wolfe AP. 2013. A first account of freshwater Potamolepid sponges (Demospongiae, Spongillina, Potamolepidae) from the middle Eocene: Biogeographic and paleoclimatic implications. Journal of Paleontology 87(3): 373-8.

Rasband WS. 1997-2015. ImageJ. U. S. National Institutes of Health.

Rohlf F. 2007. Tps series. Department of Ecology and Evolutionary Biology. Stony Brook University.

Ross R, Cox EJ, Karayeva N, Mann D, Paddock T, Simonsen R, Sims P. 1979. An amended terminology for the siliceous components of the diatom cell. Nova Hedwigia. Beiheft 64: 513-33.

Round FE, Crawford RM, Mann DG. 1990. The diatoms: Biology & morphology of the genera. First ed. United States: Cambridge University Press. 760 p.

Sims PA, Mann DG, Medlin LK. 2006. Evolution of the diatoms: Insights from fossil, biological and molecular data. Phycologia 45(4): 361-402.

Siver P, Wolfe A, Rohlf F, Shin W, Jo B. 2013. Combining geometric morphometrics, molecular phylogeny, and micropaleontology to assess evolutionary patterns in *Mallomonas* (Synurophyceae: Heterokontophyta). Geobiology 11(2): 127-38.

Siver PA and Wolfe AP. 2009. Tropical Ochrophyte algae from the Eocene of northern Canada: A biogeographic response to past global warming. Palaios 24(3): 192-8.

Siver PA and Wolfe AP. 2007. *Eunotia* spp. (Bacillariophyceae) from middle Eocene lake sediments and comments on the origin of the diatom raphe. Botany 85(1): 83-90.

Siver PA and Hamilton PB. 2011. Diatoms of North America: The freshwater flora of waterbodies on the Atlantic coastal plain. Gantner Verlag. Iconographia Diatomologica 22, 920 p.

Siver PA, Wolfe AP, Edlund MB. 2010. Taxonomic descriptions and evolutionary implications of middle Eocene pennate diatoms representing the extant genera *Oxyneis, Actinella* and *Nupela* (Bacillariophyceae). Plant Ecology and Evolution 143(3): 340-51.

Siver PA, Bishop J, Lott A, Wolfe AP. 2015. Heteropolar eunotioid diatoms (Bacillariophyceae) were common in the North American arctic during the middle Eocene. Journal of Micropaleontology 34(2): 151-63.

Steinman A and Sheath R. 1984. Morphological variability of *Eunotia pectinalis* (Bacillariophyceae) in a softwater Rhode Island stream and in culture. Journal of Phycology 20(2): 266-76.

Steinman AD and Ladewski T. 1987. Quantitative shape analysis of *Eunotia pectinalis* (Bacillariophyceae) and its application to seasonal distribution patterns. Phycologia 26(4): 467-77.

Stoermer EF and Ladewski TB. 1982. Quantitative analysis of shape variation in type and modern populations of *Gomphoneis herculeana*. Nova Hedwigia 73: 347-86.

Suto I, Jordan RW, Watanabe M. 2009. Taxonomy of middle Eocene diatom resting spores and their allied taxa from the central arctic basin. Micropaleontology: 259-312.

Theriot EC, Ruck E, Ashworth M, Nakov T, Jansen RK. 2011. Status of the pursuit of the diatom phylogeny: Are traditional views and new molecular paradigms really that different? In: The Diatom World. Seckbach J and Kociolek JP, editors. Springer. 119 p.

Wetzel C, Ector L, Hoffman L, Bicudo D. 2010. Colonial planktonic *Eunotia* (Bacillariophyceae) from Brazilian Amazon: Taxonomy and biogeographical considerations on the *E. asterionelloides* species complex. Nova Hedwigia 91: 49-86.

Wolfe AP, Edlund MB, Sweet AR, Creighton SD. 2006. A first account of organelle preservation in Eocene nonmarine diatoms: Observations and paleobiological implications. Palaios 21(3): 298-304.

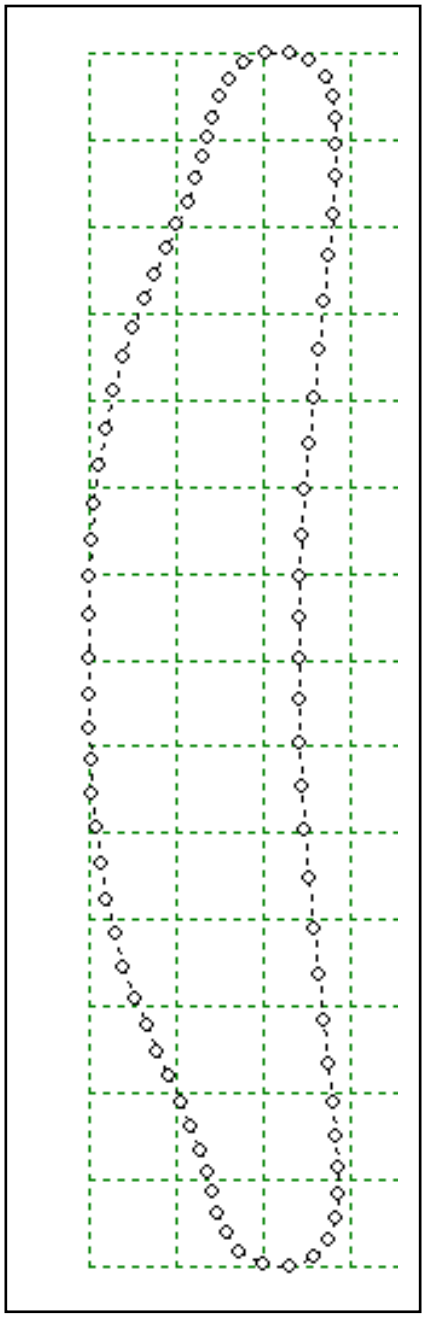

Figure 1. A thin spline grid representation of the characteristic semi-lunate valve of *Eunotia* with a marked dorsiventrality. This figure is one representation of the calculated mean, or centroid, morphology of *Eunotia* within the study displayed with a thin spline deformation grid.

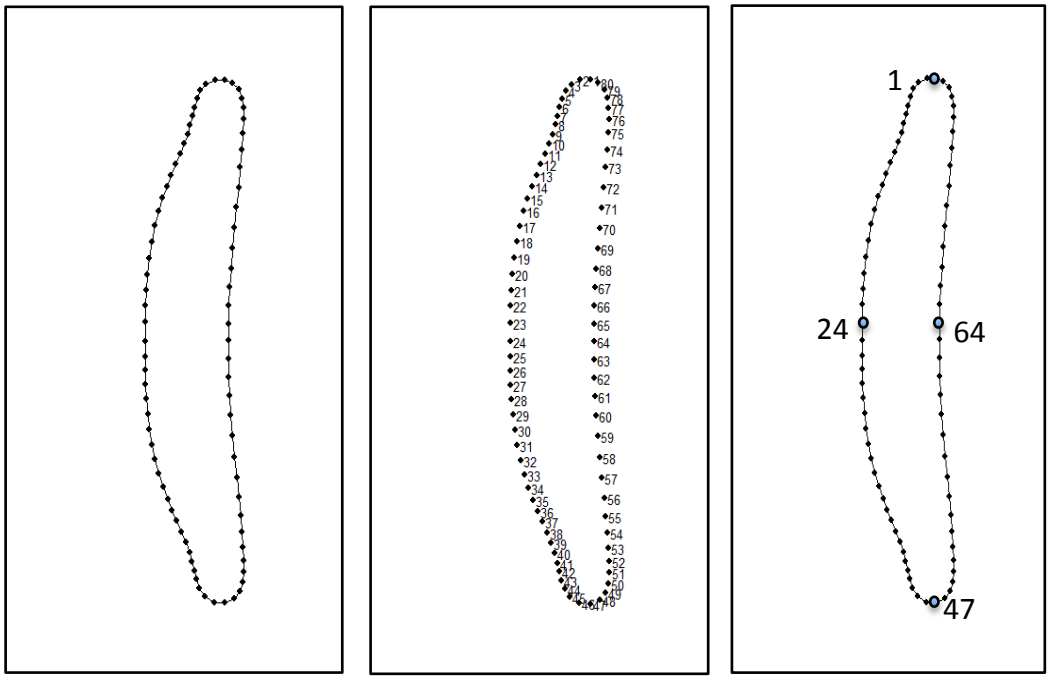

Figure 2. Mean shape, or centroid, of *Eunotia* with aligned landmark positions. All three representations display the centroid, or mean, morphology of *Eunotia* calculated from a General Procrustes Analysis for all specimens combined (N=632). The leftmost representation displays the centroid with "links" between landmarks to aid in shape visualization. The center representation displays the aligned position of all 80 landmarks used in the analysis; 76 semi-permanent, or sliding, landmarks and four permanent, non-sliding, landmarks. The latter are displayed upon the representation at the right.

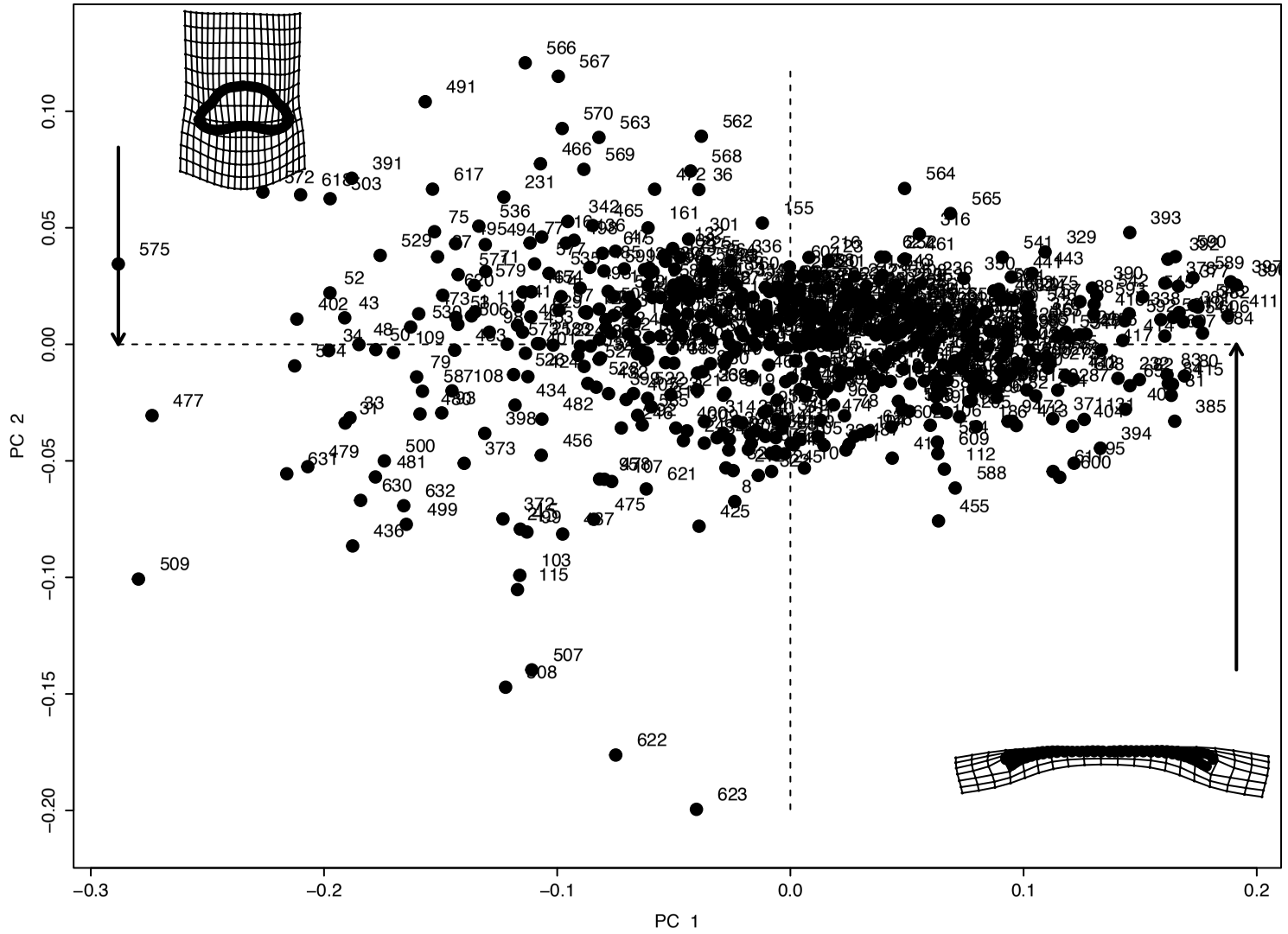

Figure 3. Result of a principal components analysis displaying the first two axes for all specimens combined (n=632). Thin spline deformations exhibited at the outermost bounds of the X-axis (PC 1) show shape transformations of specimens when traversing this axis.

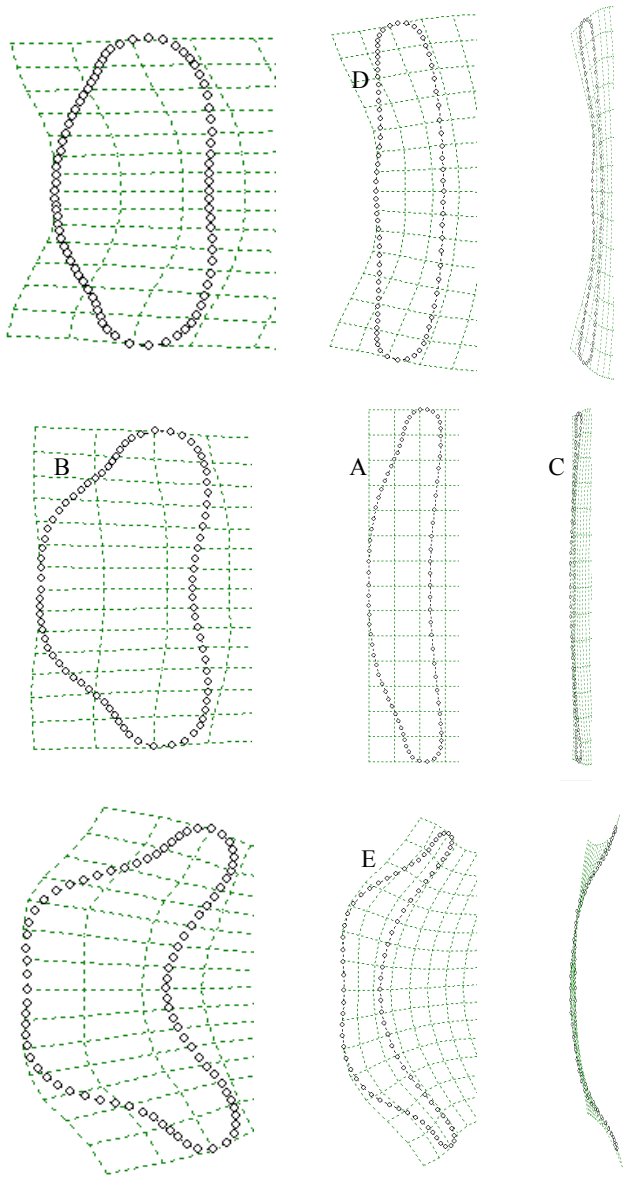

Figure 4. Thin spline diagrams displaying the change progressing along primary and secondary principal components axes after performing a generalized Procrustes alignment (GPA) with the centroid, or mean specimen, displayed at the center (A). Specimens immediately to the left (B) and right (C) represent those specimens occurring at the outermost intercepts for the primary (x) axis, whilst those immediately above (D) and below (E) are the corresponding intercepts at the extremes of the graph for the secondary (y) axis. Specimens at the corners of the plots represent the outer bounds of the graph situated between the axes.

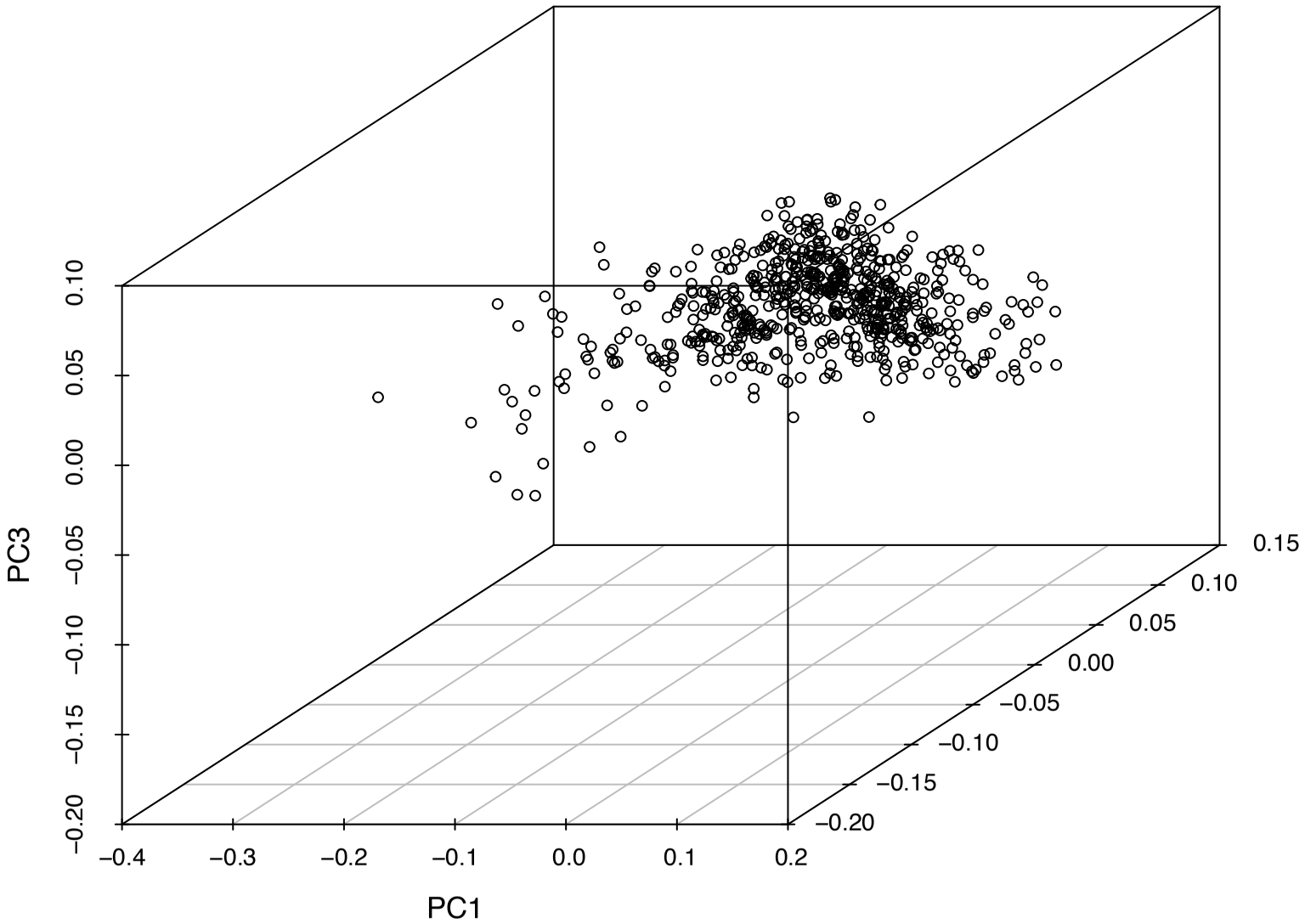

Figure 5. The results of a principal components analysis for all specimens (n=632) displaying the first three principal components axes.

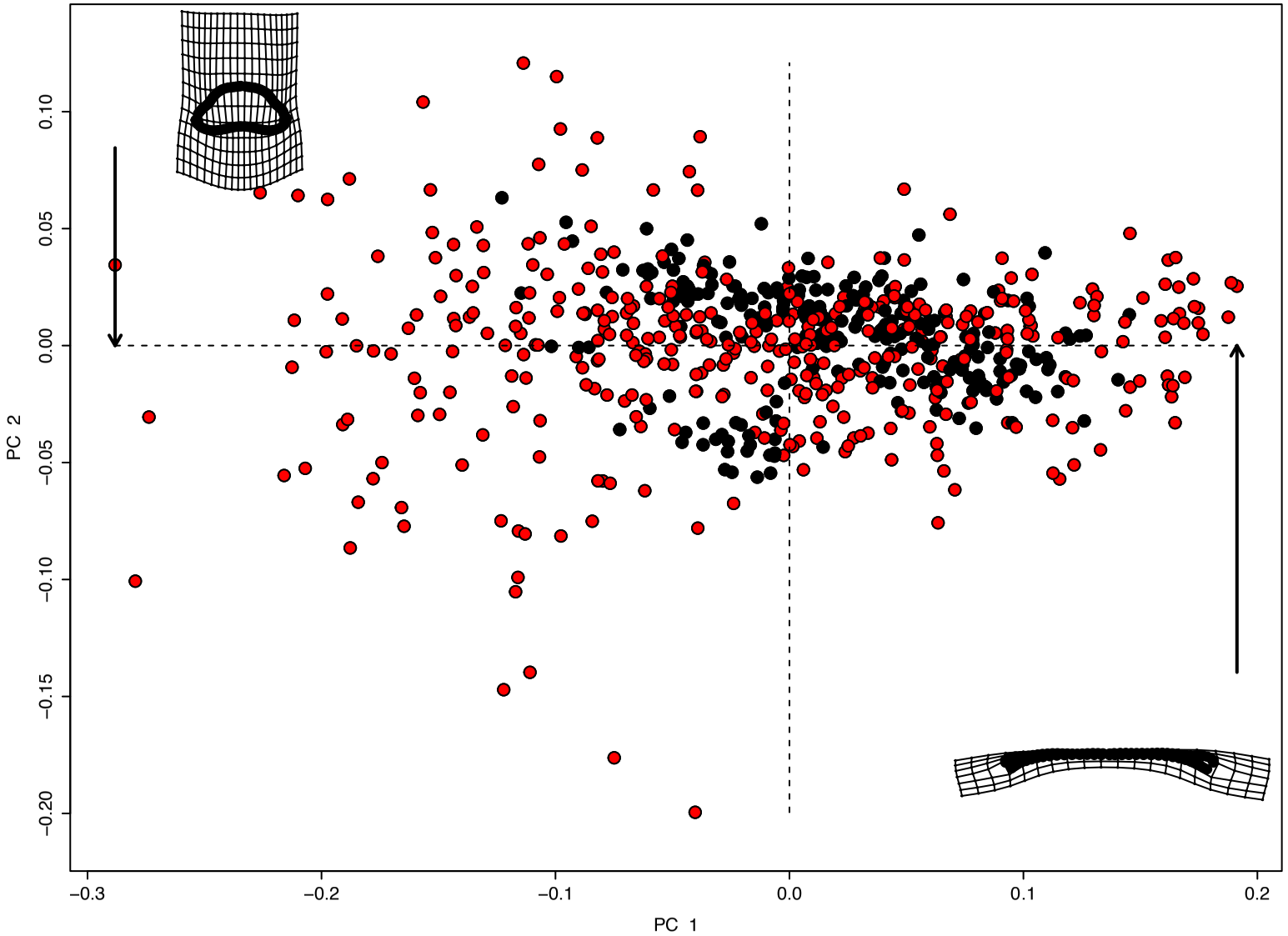

Figure 6. Results of a principal components analysis comparing extant and fossil specimens. Principal components plot displaying all specimens (n=632) further separated between extant (Red, n=384) and fossil (Black, n=248) distinctions. Here, fossil specimens from the Giraffe Pipe core are treated as a homogenous dataset, as is the global extant taxa dataset.

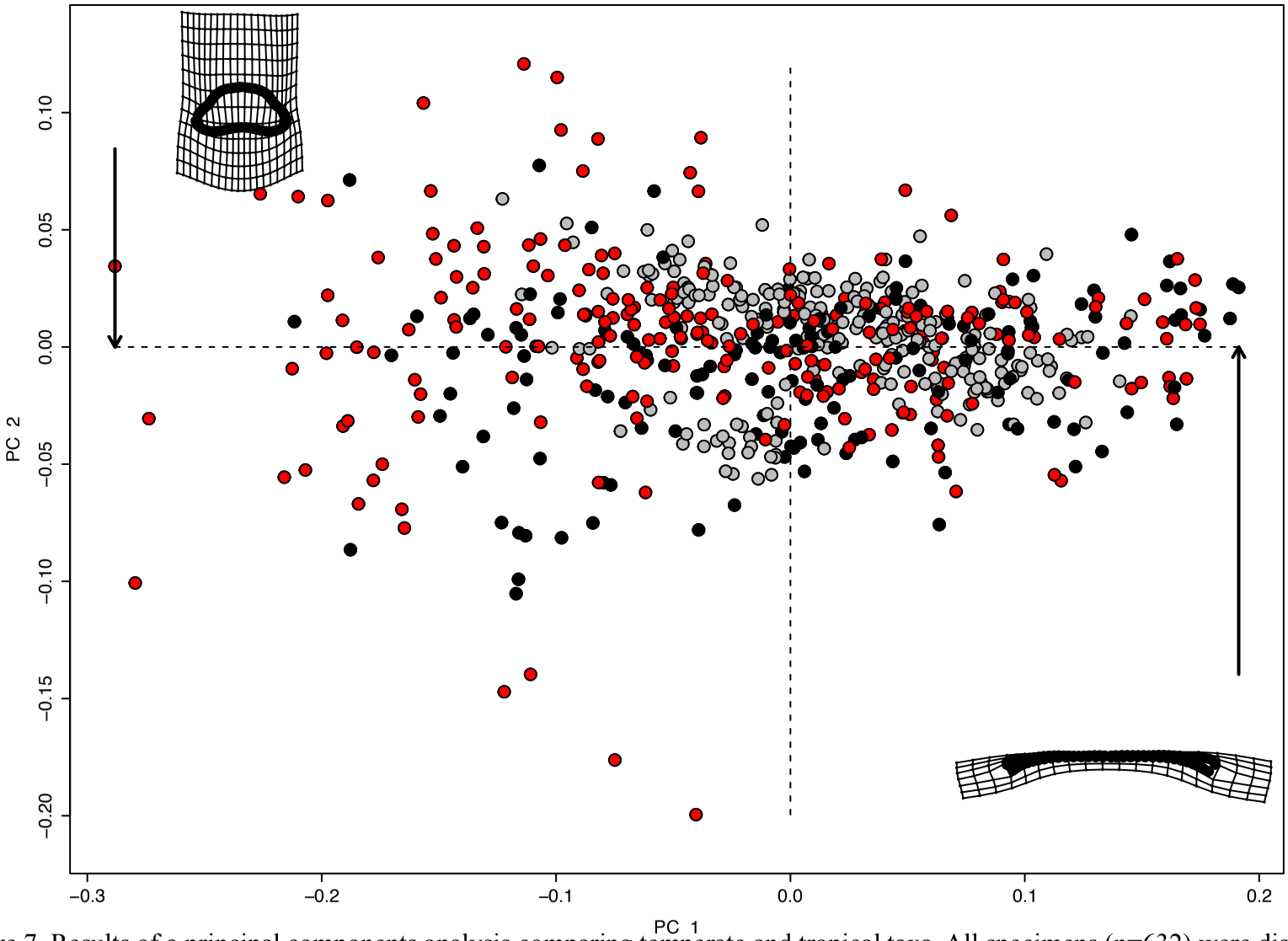

Figure 7. Results of a principal components analysis comparing temperate and tropical taxa. All specimens (n=632) were displayed against the first and second axes of the principal components and divided between temperate (Black, n=152) and tropical (Red, n=232) taxa. Fossil taxa (Grey, n=248) remain in the analysis, but are not quantified as either temperate or tropical within this analysis.

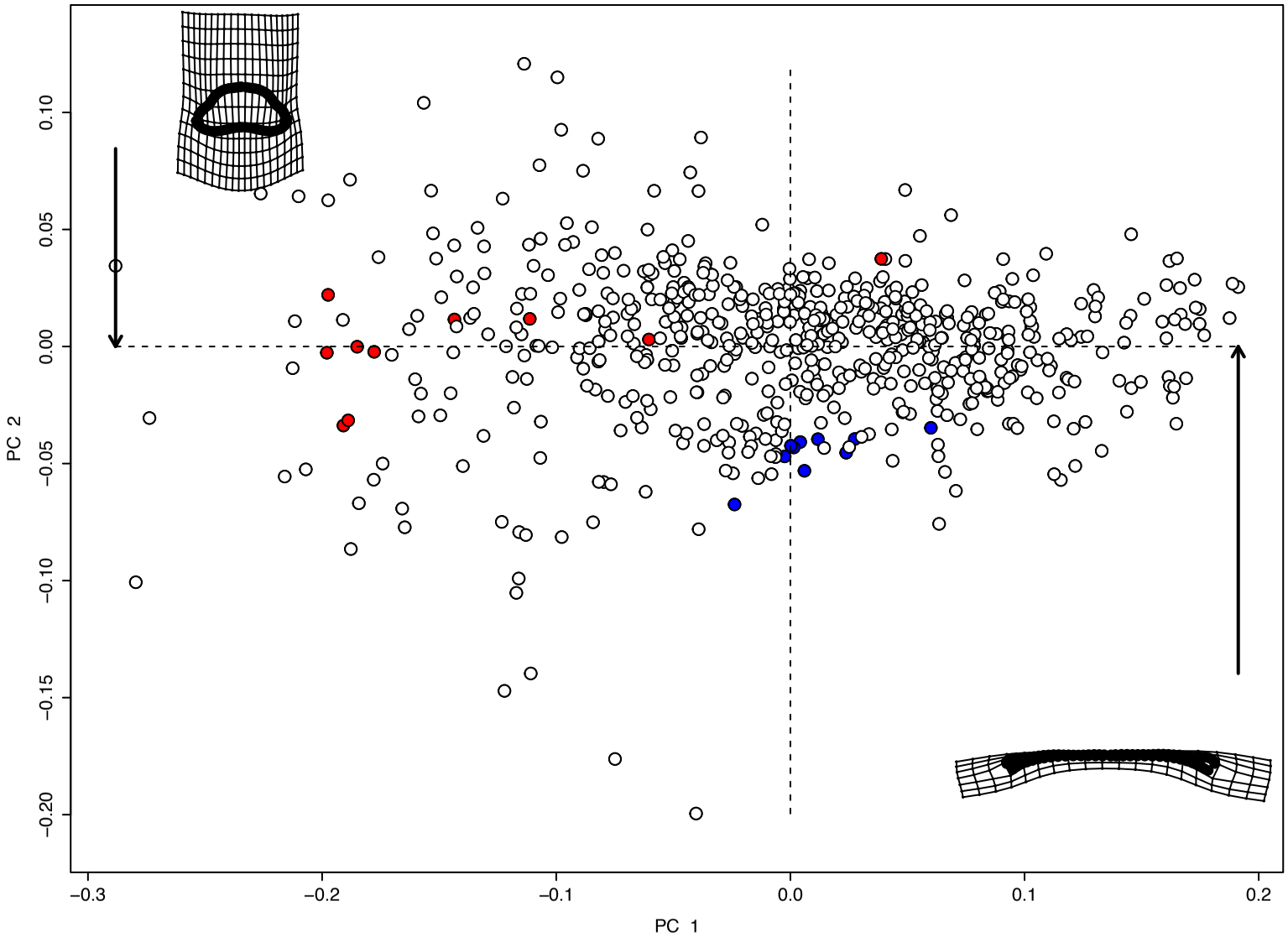

Figure 8. Results of a principal components analysis highlighting allometric trends in *Eunotia ventriosa* and *E. arcuoides*. All specimens (n=632) are displayed along the first two axes of the principal components analysis. Multiple specimens of *E. ventriosa* (Red, n=10) and *E. arcuoides* (Blue, n=10) are highlighted to show trends in allometry.

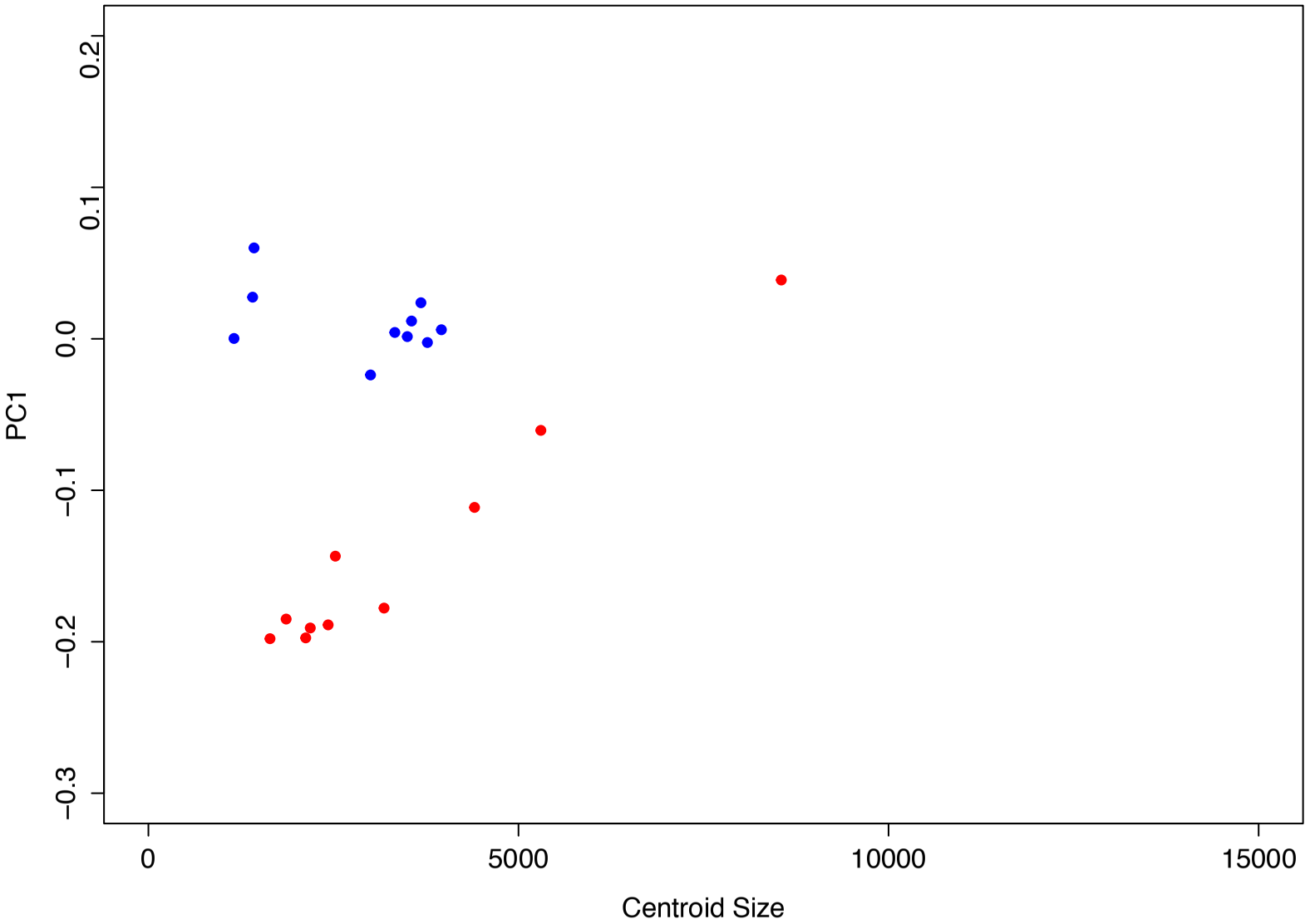

Figure 9. Allometric comparisons of 2 *Eunotia* species. Centroid size of multiple specimens of *E. ventriosa* (Red, n=10) and *E. arcuoides* (Blue, n=10) are compared against their respective scores along the first principal components axis to demonstrate shape change trajectory.

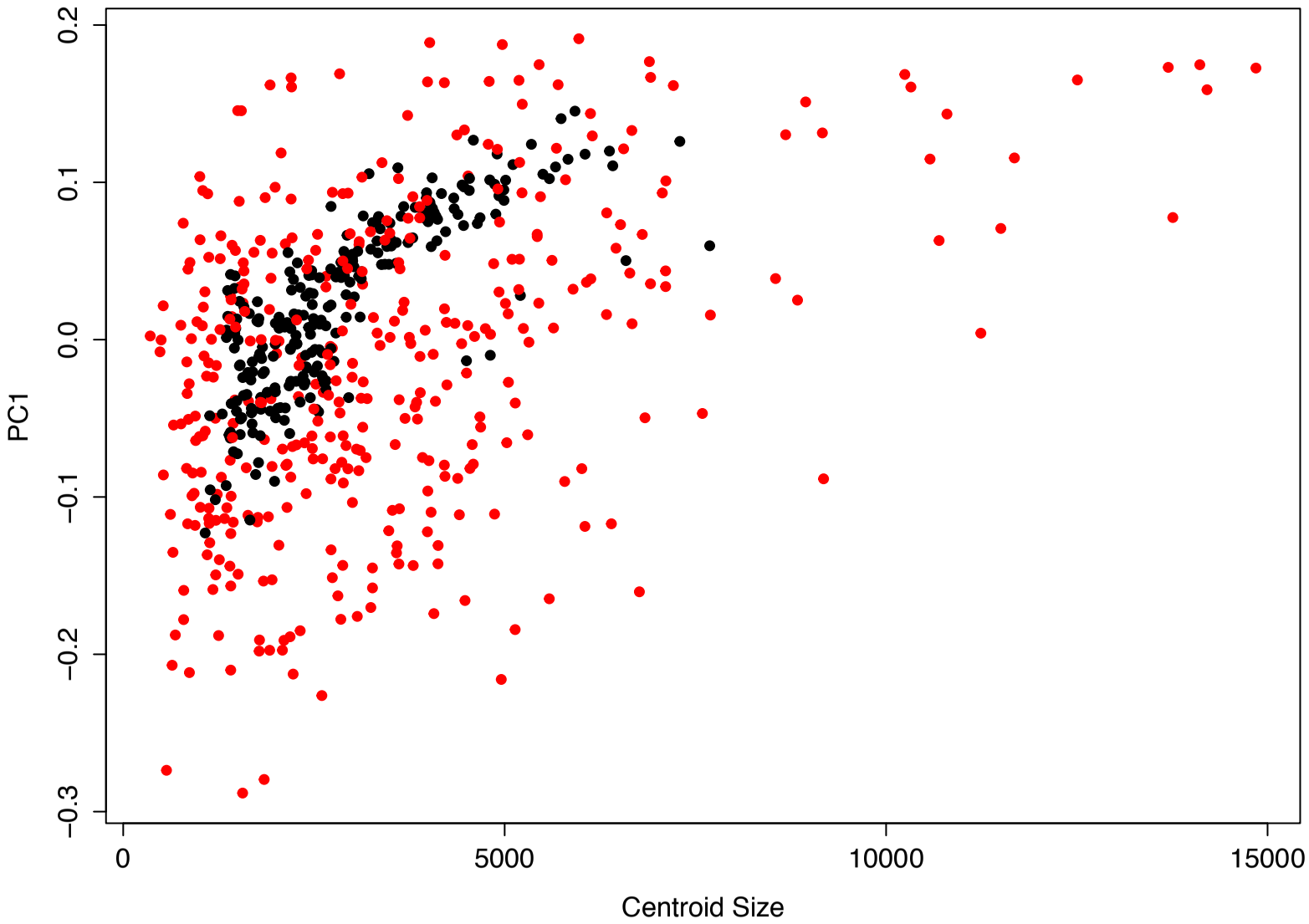

Figure 10. Shape change trajectories of *Eunotia*. All specimens (n=632) within the analysis were displayed. Centroids of fossil (black) and extant (red) specimens are compared against their respective scores from the first principal components analysis.

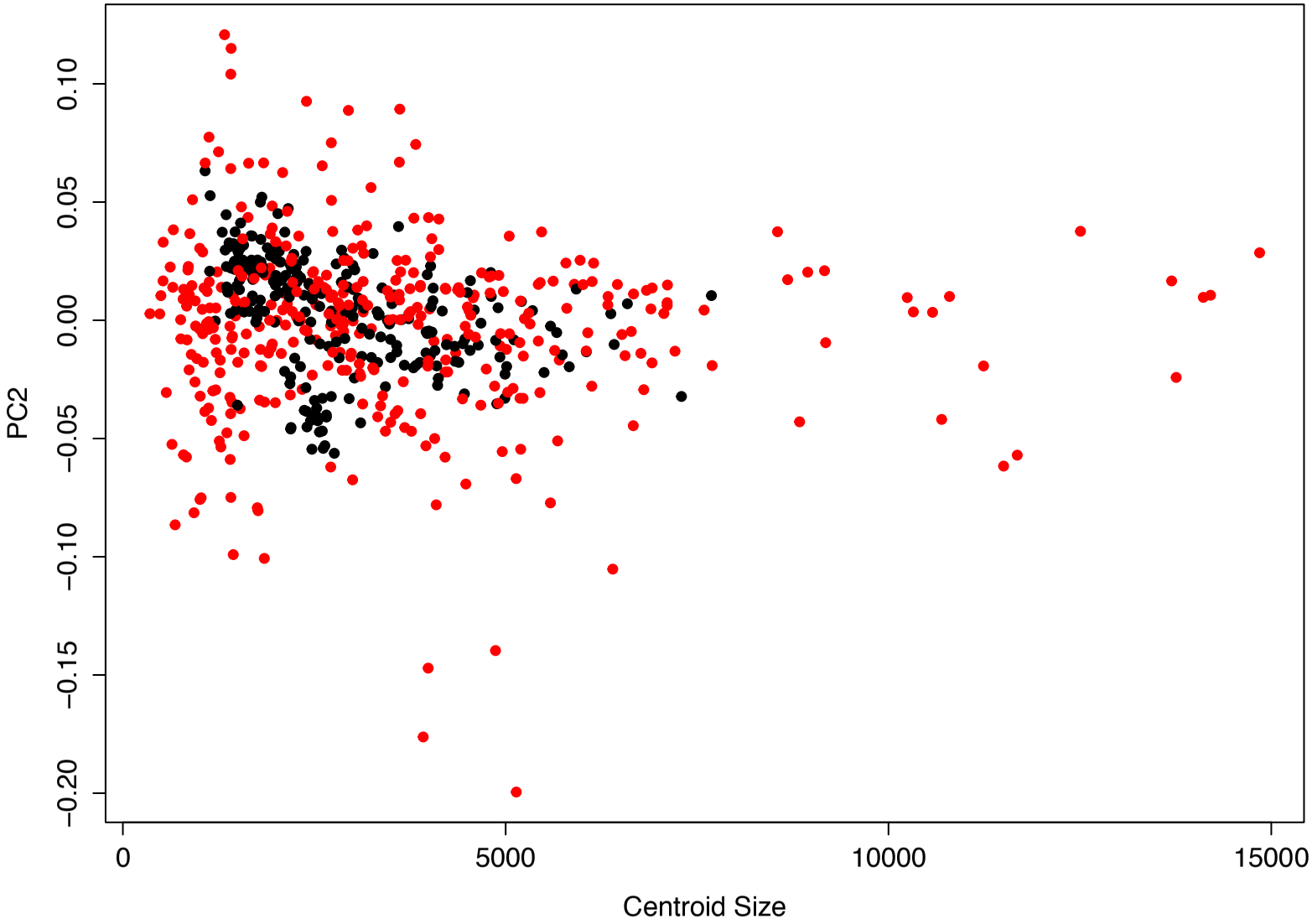

Figure 11. Shape change trajectories of *Eunotia*. All specimens (n=632) within the analysis were displayed. Centroids of fossil (black) and extant (red) specimens are compared against their respective scores from the second principal components analysis.

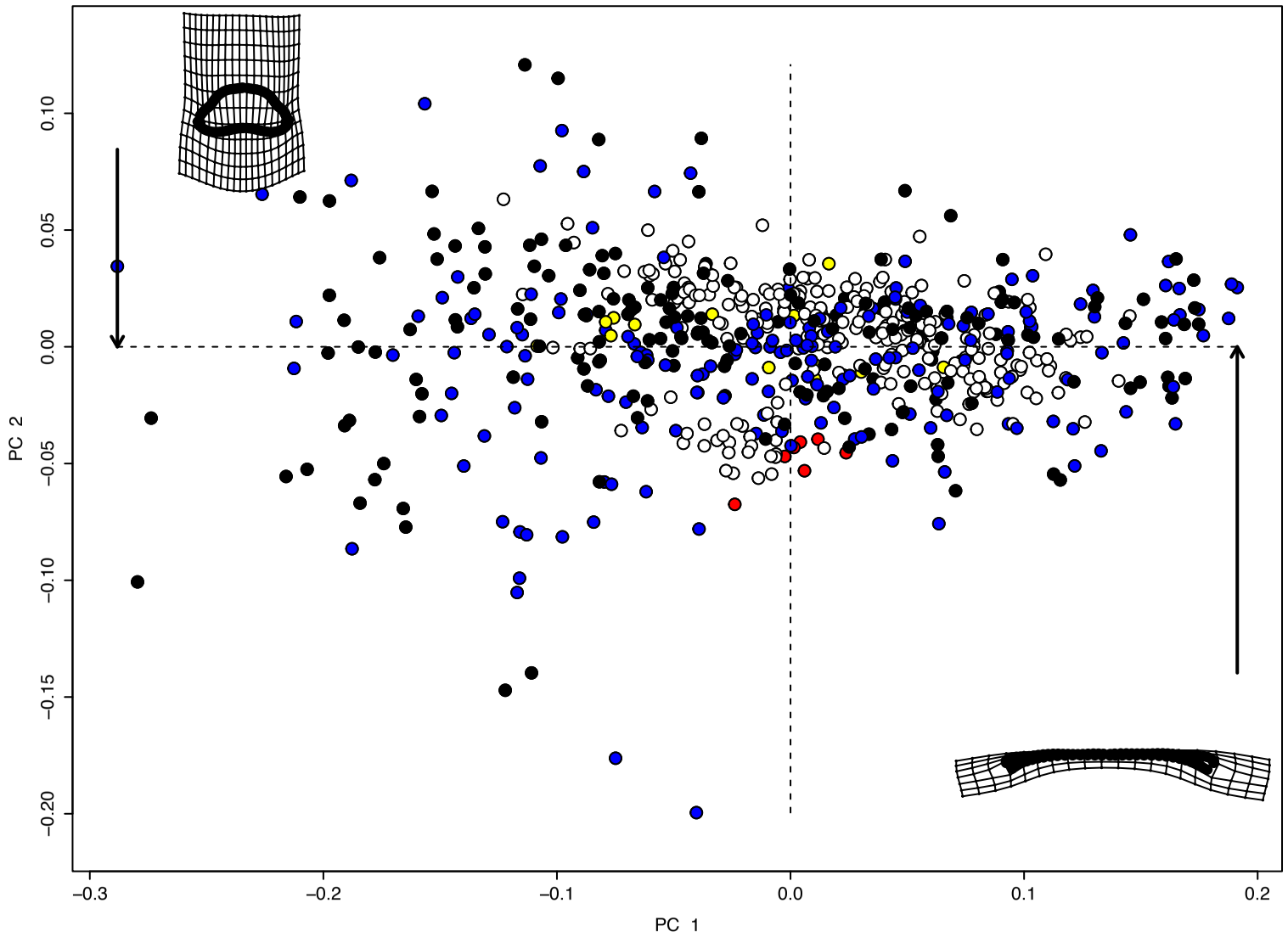

Figure 12. Results of a principal components analysis displaying specimens by their continent of origin. All specimens (n=632) are displayed and color-coded by their continent of origin. Fossil specimens are colored white and remain for comparison. African, European, North American, and South American specimens correspond to yellow, red, blue, and black respectively.

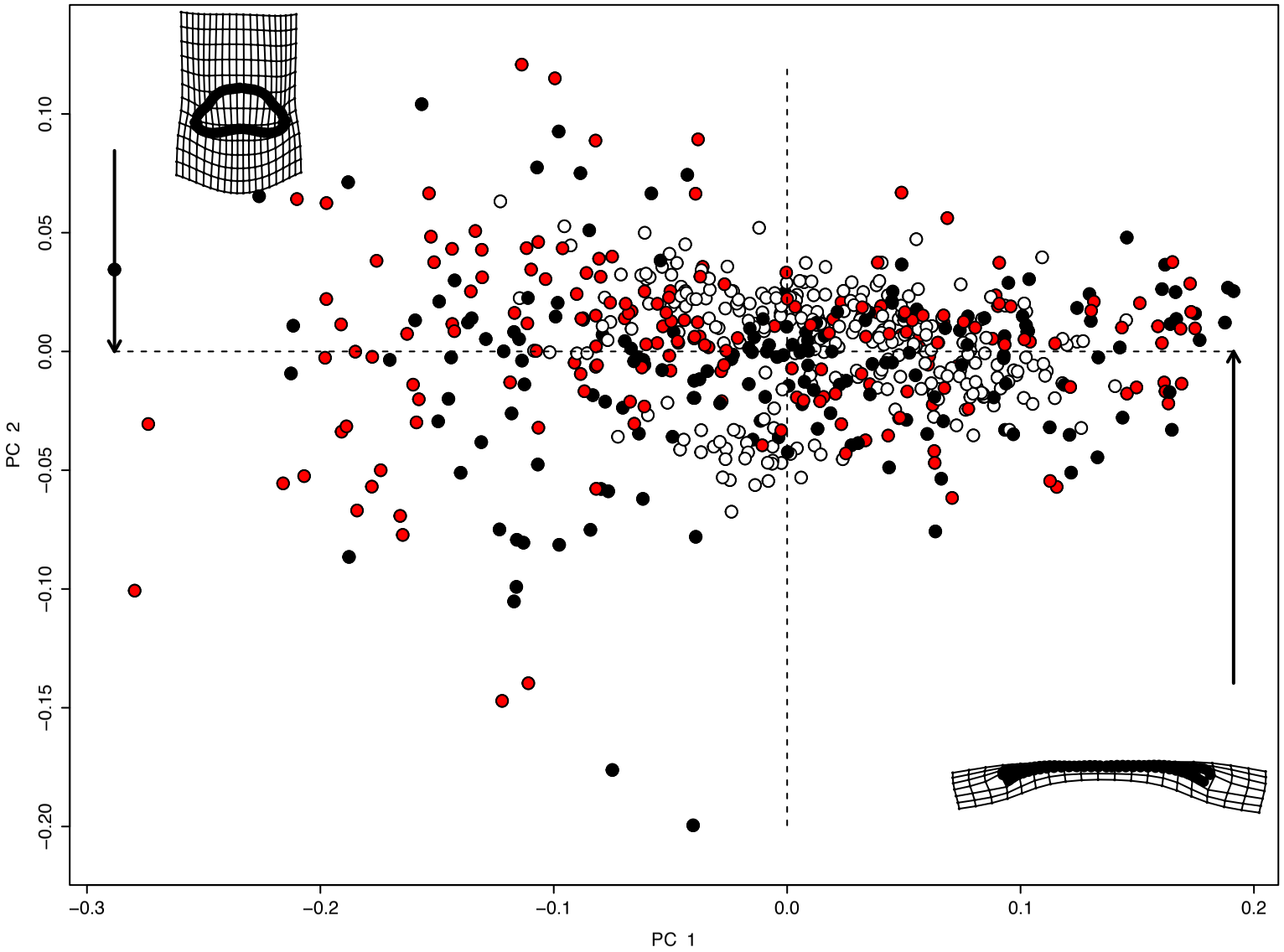

Figure 13. Results of a principal components analysis performed on all specimens (n=632) distinguishing between North and South American specimens. Fossil specimens remain in white, along with all European and African specimens. North American specimens are coded black and South American specimens are coded red.

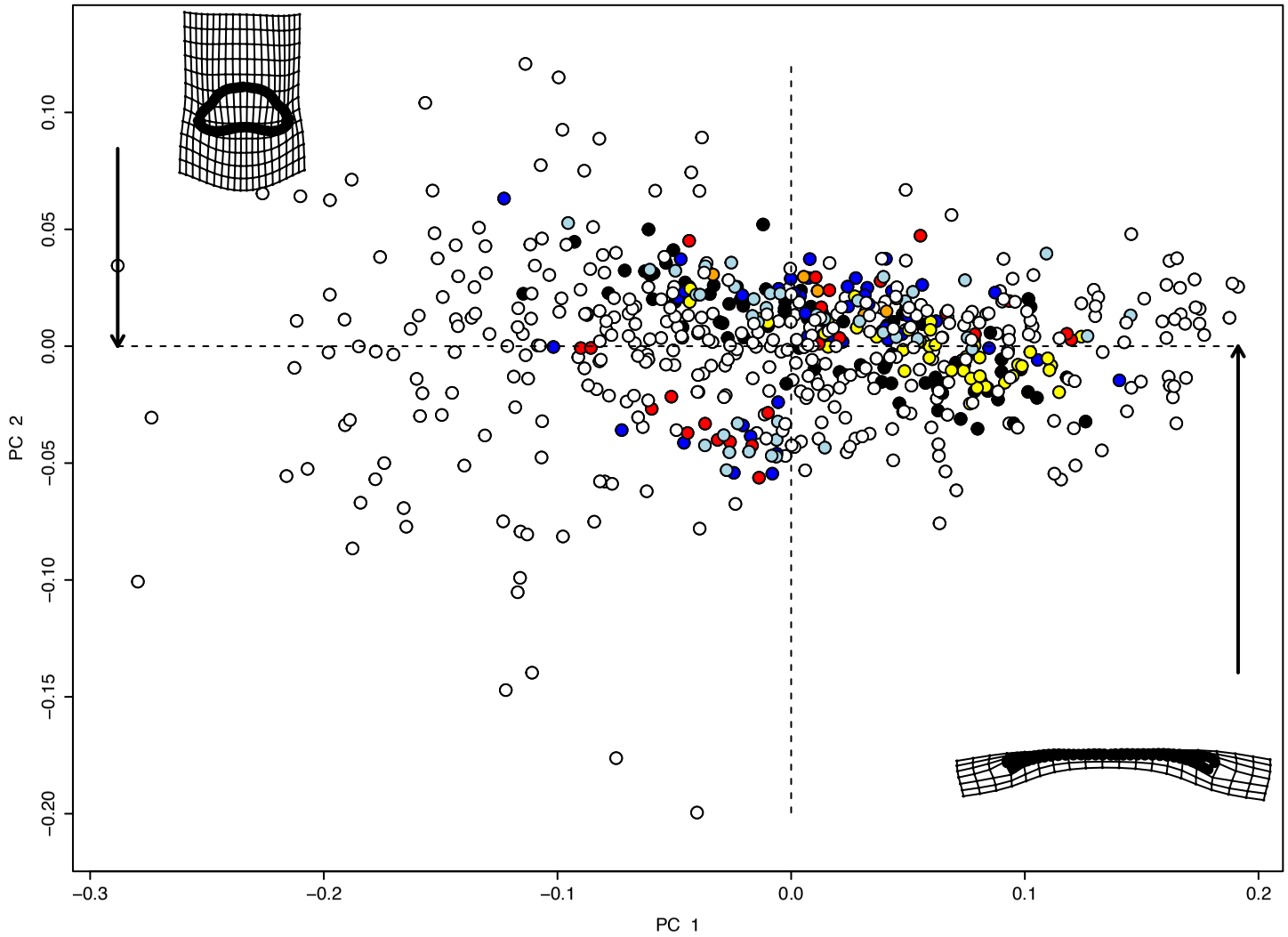

Figure 14. Results of a principal components analysis performed upon all specimens (n=632) distinguishing between fossil depths within the Giraffe Pipe sediment core. Fossil specimens are colored according to their box (sample identifier within the core) number. In the case of multiple specimens per box, the full description of box number-channel-channel depth is given. Specimens colored yellow, black, orange, blue, light blue and red correspond to specimens from boxes 11, 13, 14, 15-1-131, 15-1-65, and 16. Modern specimens here are pictured as white.

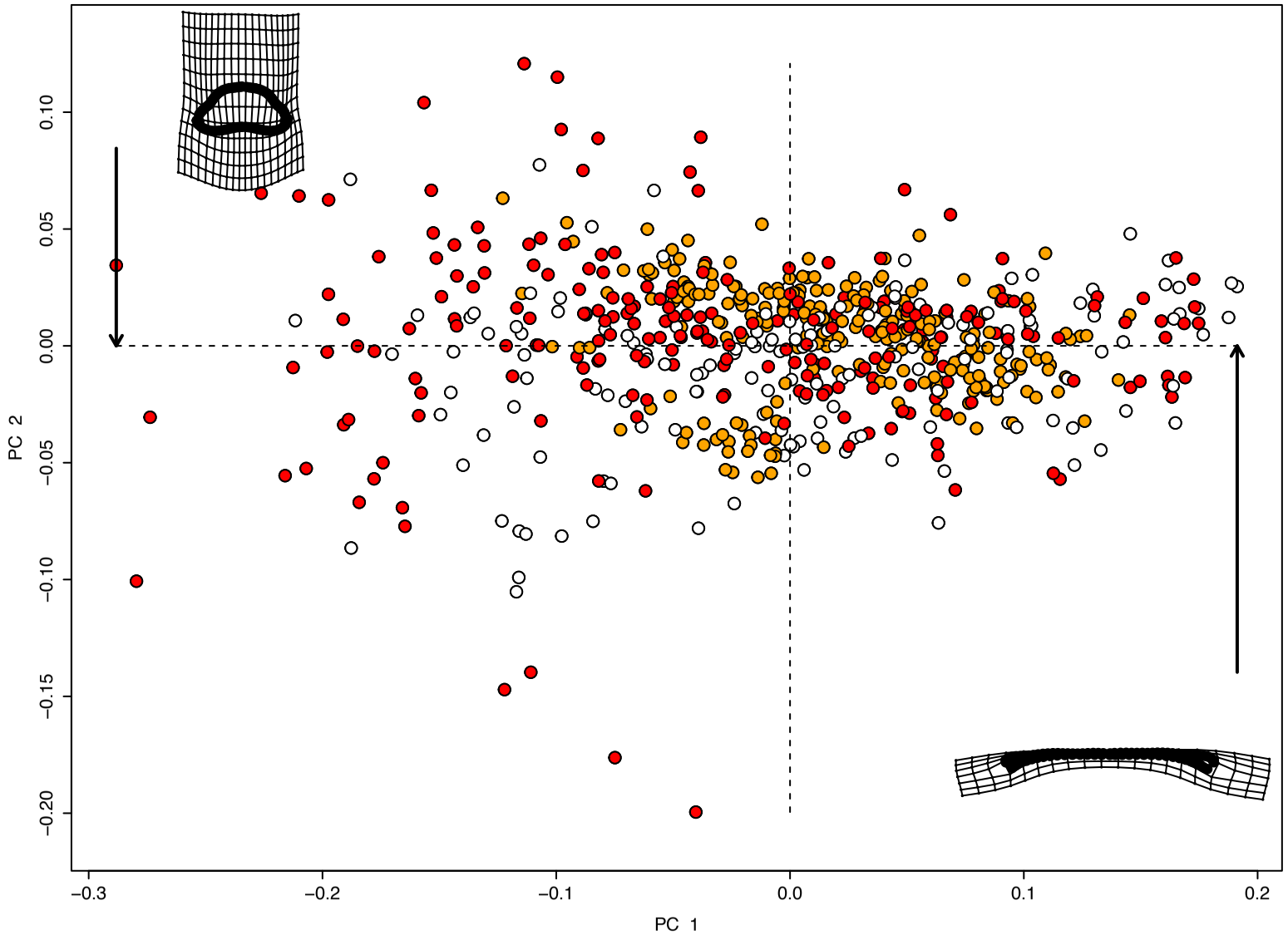

Figure 15. Results of a principal components analysis performed upon all specimens (n=632) displaying specimens color coded by tropical climate. Modern tropical taxa are compared against fossil tropical taxa, displayed in red and orange, respectively. Temperate specimens are displayed in white for comparison.

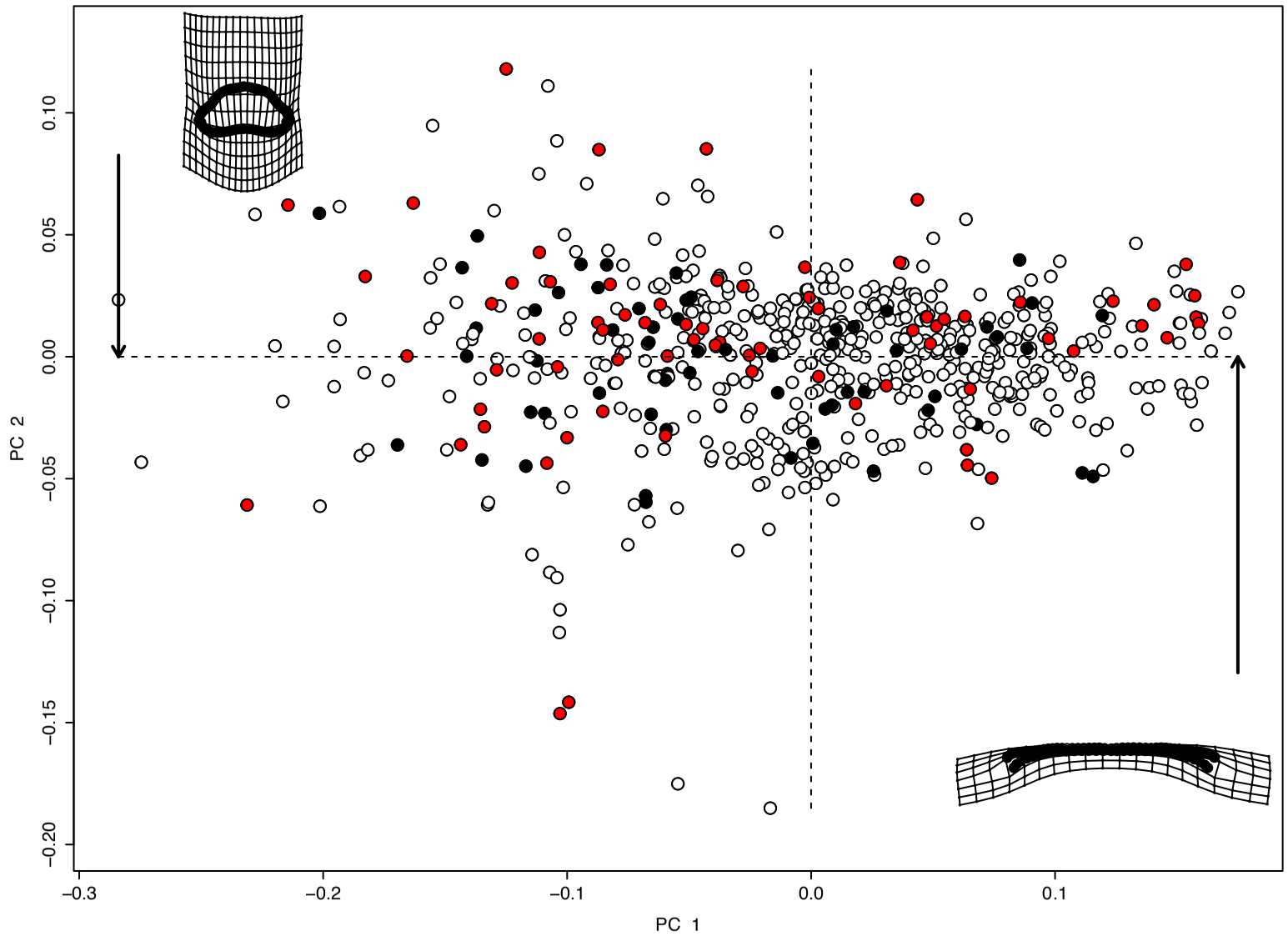

Figure 16. The result of a principal components analysis comparing planktonic and epiphytic specimens. All specimens (n=632) were included with distinctions made between planktonic (red) and epiphytic (black). Specimens lacking either of these distinctions, or unreported data are left within white to ease comparison.

Table 1. Specimens that are taxonomically categorized, by their source. Specimens from the Academy of Natural Sciences of Philadelphia at Drexel University are either type (Holotype, Syntype, Paratype) materials or taken from within the type locality. This list condenses unnamed geographic variants; though they remain identified within the analysis. There are 135 species of *Eunotia* presented. *Semiorbis hemicyclus* (n=1) was included as it is sometimes placed within *Eunotia*.

		Specimen Source				
Species Number	*Eunotia spp.* (Unless otherwise designated)	Patrick & Reimer (1966)	Siver& Hamilton (2011)	ANSP Online Herbarium Holdings	Metzeltin (2009)	ANSP General Collection
1	*acicularis*		1			
2	*acutinasuta*				3	
3	*acutirenulata*				4	
4	*aduncus*			1		
5	*americana*			1		
6	*arcuoides*			3		7
7	*baculus*				2	
8	*bidens*				5	
9	*bilii*			3		1
10	*bilunaris*		2			
11	*biseriata*				1	
12	*buhriana*				2	
13	*camburnii*				2	
14	*camelus*		2			
15	*carolina*	1	3	2		
16	*catiliferra*				1	
17	*charlesii*				2	
18	*comica*				2	
19	*convexa*				3	
20	*convexa form. impressa*				2	
21	*copiosa*				1	
22	*crassula*				3	
23	*croatana*		2			
24	*curvula*				1	
25	*denticulata*				2	
26	*disjuncta*				4	
27	*donatoi*				1	
28	*edlundii*				3	
29	*elucens*				3	
30	*fabeola*				3	
31	*femoriforme*		2			
32	*floridana*				2	
33	*floweri*				2	
34	*heinii*				2	
35	*hillae*				3	
36	*hirudo*				3	
37	*incisiopsis*				2	
38	*indica*	1				
39	*informis*				3	
40	*katalinae*				3	
41	*kissii*				3	
42	*lapponica*	1				

Table 1. Continued.

43	*levicrenulata*				2	
44	*lewisii*		2			
45	*luna*	1				
46	*machaon*				3	
47	*maior*	1				
48	*maior var. ventricosa*	1				
49	*meisteri*	1				
50	*meridiana*				3	
51	*microcephala*	1				
52	*monodon*	1				
53	*monodon var. constricta*	1				
54	*naegelii*	1	2			
55	*napoleonica*				3	
56	*neglecta*				3	
57	*nivalis*			1		
58	*noerpeliana*				1	
59	*nymanniana*	1				
60	*obesa var. wardii*	1				
61	*obtusa*				3	
62	*paludosa*				2	
63	*parallela*	1				
64	*patrickae*				3	
65	*paucistriata*				2	
66	*pauloimpressa*				3	
67	*paulovalida*				2	
68	*pectinalis*	2	4			
69	*pectinalis var. biarcuata*		1			
70	*pectinalis var. minor*	2				
71	*pectinalis var. recta*	1				
72	*pectinalis var. ventricosa*	1				
73	*perctinalis var. undulata*	1				
74	*perminuta*	2				
75	*perpusilla*	1				
76	*pocosinensis*			2		
77	*praerupta*	1				
78	*praerupta var. bidens*	1				
79	*praerupta var. monodon form. polaris*		1			
80	*praerupta var. inflata*	1				
81	*pseudofragilaria*		2			
82	*punctastriata*				2	1
83	*quadra*		2			
84	*quaternaria*	1				
85	*rabenhorstiana*				3	
86	*rabenhorstii var. monodon*					
87	*reimeri*			1		
88	*rolandschmidtii*				3	
89	*romanowi*		2			
90	*rostellata*	1				
91	*sarraceniae*			2		
92	*Semiorbis hemicyclus*				2	
93	*septentrionalis*	1				

Table 1. Continued.

94	*serra*	1	3	4	
95	*serra var. diadema*	1			
96	*sinuosa*			1	
97	*siveri*			3	
98	*soleirolii*	1			
99	*species 2*		1		
100	*sphagnophila*			3	
101	*stevenosonii*			1	
102	*subarcuatoides*		1		
103	*subrosta*			1	
104	*sudetica*	1			
105	*suecica*	1			
106	*sulcatoides*			3	
107	*tambaquina*			3	
108	*tanosoensis*				1
109	*tapacuminor*			3	
110	*tauntoniensis*		2		
111	*tenella*	1			
112	*tenuivalva*			1	
113	*tridentula*			3	
114	*trinacria*	1			
115	*trinacria var.undulata*	1			
116	*triodon*	1			
117	*tropicoarcus*			3	
118	*undulata*			1	
119	*usteri*			2	
120	*valida*	1			
121	*vanheurckii*	1			
122	*vanheurckii var. intermedia*	1			
123	*vasta*			1	
124	*veneris*			1	
125	*veneroides*			2	
126	*ventriosa*			3	7
127	*ventriosa var. brevis*			3	
128	*veroformosa*			2	
129	*vinculi*		1		
130	*winsboroughae*			3	
131	*yanomami*		2	1	
132	*zizkae*			3	
133	*zygodon*	1			

Table 2. The corrected vertical depths of samples within the Giraffe Pipe, drilled at a 47 degree angle. Lake depth approximates the water depth on which the sample was taken. Complete number of specimens per each sample are given. Specimens were photographed from a single slide, unless otherwise noted. Adopted from Siver et al., 2010.

Box Number	Corrected Depth (m)	Depth in Lake (m)	Number of specimens
11-3-90	70.09	0.51	41
13-2-120	78.14	8.56	89
14-2-56	80.96	11.38	5
15-1-65	85.41	15.83	42
15-1-131	85.9	16.32	47
16-3-81	86.63	17.05	24

Table 3. Results of a principal components analysis displaying the proportion of variance and cumulative proportion explained by the first ten axes.

	PC1	PC2	PC3	PC4	PC5	PC6	PC7	PC8	PC9	PC10
Proportion of Variance	0.72808	0.10367	0.04061	0.02454	0.0195	0.01291	0.00756	0.00705	0.00632	0.00558
Cumulative Proportion	0.72808	0.83175	0.87236	0.8969	0.9164	0.92931	0.93687	0.94392	0.95024	0.95582
Standard Deviation	0.08651	0.03264	0.02043	0.01588	0.01416	0.01152	0.008816	0.00851	0.008057	0.007576

Table 4. The results of linear regressions comparing Log(10) transformed data against valve measurements and results of the principal components analysis for all specimens (N=632).

Variables	Multiple r squared	Adjusted r squared	p Value	n	Df	Dataset
Raw Length vs. Raw Length	0.2251	0.2239	< 2.2e-16	632	630	All specimens
Log Length vs. Log Width	0.1981	0.1968	< 2.2e-16	632	630	All specimens
Log LW vs PC1	0.8668	0.8666	< 2.2e-16	632	630	All specimens
Log LW vs PC2	0.007821	0.006246	0.0262	632	630	All specimens
Log LW vs PC3	0.004862	0.003283	0.07984	632	630	All specimens
Log LW vs PC4	0.0006625	-0.0009238	0.5184	632	630	All specimens
Raw Length vs PC1	0.199	0.1977	< 2.2e-16	632	630	All specimens
Raw Length vs PC2	0.0561	0.0546	1.66E-09	632	630	All specimens
Raw Length vs PC3	0.01532	0.01376	0.001825	632	630	All specimens
Raw Length vs PC4	0.007953	0.06379	2.50E-02	632	630	All specimens
Log Length vs. PC1	0.2559	0.2547	< 2.2e-16	632	630	All Specimens
Log Length vs. PC2	0.09364	0.0922	3.63E-15	632	630	All Specimens
Log Length vs. PC3	0.02395	0.0224	9.37E-05	632	630	All Specimens
Log Length vs. PC4	0.001193	-0.0003929	3.86E-01	632	630	All Specimens
Raw Width vs. PC1	0.1753	0.174	< 2.2e-16	632	630	All specimens
Raw Width vs. PC2	0.07111	0.06964	9.47E-12	632	630	All specimens
Raw Width vs. PC3	2.51E-03	0.0009299	0.2082	632	630	All specimens
Raw Width vs. PC4	0.01193	0.01036	5.98E-03	632	630	All specimens
Log Width vs. PC1	0.2282	0.227	< 2.2e-16	632	630	All specimens
Log Width vs. PC2	0.06009	0.0586	5.86E-04	632	630	All specimens
Log Width vs. PC3	0.009175	0.007603	1.60E-02	632	630	All specimens
Log Width vs. PC4	0.004599	0.003019	8.85E-02	632	630	All specimens
Raw Ventral Length vs. PC1	0.0001032	-0.001484	0.7988	632	630	All specimens
Raw Ventral Length vs. PC2	9.51E-04	-0.0006346	0.4389	632	630	All specimens
Raw Ventral Length vs. PC3	0.0002128	-0.001374	0.7144	632	630	All specimens
Raw Ventral Length vs. PC4	1.63E-05	-0.001571	0.9193	632	630	All specimens
Log Ventral Length vs. PC1	0.1443	0.1429	< 2.2e-16	632	630	All specimens
Log Ventral Length vs. PC2	0.06353	0.06204	1.29E-10	632	630	All specimens
Log Ventral Length vs. PC3	0.01749	0.01593	0.0008592	632	630	All specimens
Log Ventral Length vs. PC4	0.001878	0.0002934	2.77E-01	632	630	All specimens
Raw Dorsal Length vs. PC1	0.01495	0.01339	0.002071	632	630	All specimens
Raw Dorsal Length vs. PC2	0.001657	7.27E-05	0.3069	632	630	All specimens
Raw Dorsal Length vs. PC3	0.01034	0.008773	0.01052	632	630	All specimens

Table 4. Continued.

Raw Dorsal Length vs. PC4	2.69E-03	0.001111	0.1925	632	630	All specimens
Log Dorsal Length vs. PC1	0.08378	0.08233	1.16E-13	632	630	All specimens
Log Dorsal Length vs. PC2	0.1151	0.1137	< 2.2e-16	632	630	All specimens
Log Dorsal Length vs. PC3	0.03783	0.0363	8.35E-07	632	630	All specimens
Log Dorsal Length vs. PC4	0.00464	0.00306	8.71E-02	632	630	All specimens
Log DV vs. PC1	0.02205	0.02049	1.80E-04	632	630	All specimens
Log DV vs. PC2	0.007227	0.005651	0.03261	632	630	All specimens
Log DV vs. PC3	4.27E-03	0.002687	0.1008	632	630	All specimens
Log DV vs. PC4	7.22E-04	-0.0008638	0.5	632	630	All specimens
Log DL vs. PC1	0.1134	0.112	< 2.2e-16	632	630	All specimens
Log DL vs. PC2	0.01587	0.0143	1.51E-03	632	630	All specimens
Log DL vs. PC3	0.01214	0.01057	0.00556	632	630	All specimens
Log DL vs. PC4	0.005538	0.003959	0.06153	632	630	All specimens
Log VL vs. PC1	0.00581	0.004232	0.05546	632	630	All specimens
Log VL vs. PC2	7.42E-05	-0.001513	0.8288	632	630	All specimens
Log VL vs. PC3	1.47E-05	-0.001573	0.9233	632	630	All specimens
Log VL vs. PC4	0.0005764	-0.00101	0.5469	632	630	All specimens

Table 5. The results of linear regressions comparing Log(10) transformed data against valve measurements and results of the principal components analysis for extant, temperate specimens (N=152).

Variables	Multiple r squared	Adjusted r squared	p Value	n	Df	Dataset
Log Length vs. Log Width	0.2459	0.2409	8.23E-11	152	150	Extant temperate
Log LW vs PC1	0.8787	0.8778	< 2.2e-16	152	150	Extant temperate
Log LW vs PC2	0.028	0.02152	0.03935	152	150	Extant temperate
Log LW vs PC3	1.82E-01	0.1761	4.43E-08	152	150	Extant temperate
Log LW vs PC4	0.01882	0.01228	0.09194	152	150	Extant temperate
Log Length vs. PC1	0.2542	0.2493	3.53E-11	152	150	Extant temperate
Log Length vs. PC2	0.04505	0.03868	0.00866	152	150	Extant temperate
Log Length vs. PC3	0.005391	-0.00124	0.3687	152	150	Extant temperate
Log Length vs. PC4	0.004584	-0.002052	0.4072	152	150	Extant temperate
Log Width vs. PC1	0.1901	0.1847	1.97E-08	152	150	Extant temperate
Log Width vs. PC2	0.1578	0.1521	4.06E-07	152	150	Extant temperate
Log Width vs. PC3	0.1315	0.1257	4.42E-06	152	150	Extant temperate
Log Width vs. PC4	0.04542	0.03905	0.008387	152	150	Extant temperate
Log Ventral Length vs. PC1	0.09001	0.08394	0.0001732	152	150	Extant temperate
Log Ventral Length vs. PC2	0.01549	0.008928	0.1266	152	150	Extant temperate
Log Ventral Length vs. PC3	0.004744	-0.001891	0.3992	152	150	Extant temperate
Log Ventral Length vs. PC4	0.001998	-0.004655	0.5845	152	150	Extant temperate
Log Dorsal Length vs. PC1	0.1556	0.15	4.95E-07	152	150	Extant temperate
Log Dorsal Length vs. PC2	0.08138	0.07525	0.0003676	152	150	Extant temperate
Log Dorsal Length vs. PC3	0.0007817	-0.00588	0.7324	152	150	Extant temperate
Log Dorsal Length vs. PC4	0.01223	0.005649	0.1749	152	150	Extant temperate
Log DV vs. PC1	7.06E-05	-0.006596	0.9182	152	150	Extant temperate
Log DV vs. PC2	0.02032	0.01379	0.07976	152	150	Extant temperate
Log DV vs. PC3	0.00493	-0.001704	0.39	152	150	Extant temperate
Log DV vs. PC4	3.65E-03	-0.00299	0.4596	152	150	Extant temperate
Log DL vs. PC1	0.6718	0.6696	< 2.2e-16	152	150	Extant temperate
Log DL vs. PC2	0.1902	0.1848	1.95E-08	152	150	Extant temperate
Log DL vs. PC3	0.09589	0.08986	0.0001036	152	150	Extant temperate
Log DL vs. PC4	0.07177	0.06558	0.0008472	152	150	Extant temperate
Log VL vs. PC1	0.02336	0.01685	0.06013	152	150	Extant temperate
Log VL vs. PC2	0.004478	-0.002159	0.4127	152	150	Extant temperate
Log VL vs. PC3	0.0002514	-0.006414	0.8463	152	150	Extant temperate
Log VL vs. PC4	0.0001886	-0.006477	0.8666	152	150	Extant temperate

Table 6. The results of linear regressions comparing Log(10) transformed data against valve measurements and results of the principal components analysis for extant, tropical specimens (N=232).

Variables	Multiple r squared	Adjusted r squared	p Value	n	Df	Dataset
Log Length vs. Log Width	0.1154	0.1115	1.13E-07	232	230	Extant tropical
Log LW vs PC1	0.8807	0.8802	< 2.2e-16	232	230	Extant tropical
Log LW vs PC2	0.01073	0.006425	0.1157	232	230	Extant tropical
Log LW vs PC3	0.02457	0.02033	0.01687	232	230	Extant tropical
Log LW vs PC4	0.000561	-0.003784	0.7197	232	230	Extant tropical
Log Length vs. PC1	0.3088	0.3057	2.20E-16	232	230	Extant tropical
Log Length vs. PC2	0.08267	0.07868	8.58E-06	232	230	Extant tropical
Log Length vs. PC3	0.0004316	-0.003914	0.7529	232	230	Extant tropical
Log Length vs. PC4	0.003274	-0.001059	0.3856	232	230	Extant tropical
Log Width vs. PC1	0.2747	0.2715	< 2.2e-16	232	230	Extant tropical
Log Width vs. PC2	0.03712	0.03294	0.003214	232	230	Extant tropical
Log Width vs. PC3	0.028	0.02377	0.01069	232	230	Extant tropical
Log Width vs. PC4	0.001198	-0.003145	0.6	232	230	Extant tropical
Log Ventral Length vs. PC1	0.2034	0.1999	5.05E-13	232	230	Extant tropical
Log Ventral Length vs. PC2	0.06395	0.05988	9.85E-05	232	230	Extant tropical
Log Ventral Length vs. PC3	0.0005635	-0.003782	0.7191	232	230	Extant tropical
Log Ventral Length vs. PC4	0.0007059	-0.003639	6.87E-01	232	230	Extant tropical
Log Dorsal Length vs. PC1	0.05487	0.05076	0.0003196	232	230	Extant tropical
Log Dorsal Length vs. PC2	0.09443	0.09049	1.83E-06	232	230	Extant tropical
Log Dorsal Length vs. PC3	0.007902	0.003589	0.1772	232	230	Extant tropical
Log Dorsal Length vs. PC4	3.03E-06	-0.004345	9.79E-01	232	230	Extant tropical
Log DV vs. PC1	0.05198	0.04785	0.0004654	232	230	Extant tropical
Log DV vs. PC2	0.00405	-0.0002798	0.3345	232	230	Extant tropical
Log DV vs. PC3	0.01492	0.01063	0.06328	232	230	Extant tropical
Log DV vs. PC4	0.0009208	-0.003423	0.6457	232	230	Extant tropical
Log DL vs. PC1	0.09431	0.09037	1.86E-06	232	230	Extant tropical
Log DL vs. PC2	0.01383	0.00954	0.07383	232	230	Extant tropical
Log DL vs. PC3	0.02452	0.02028	0.01699	232	230	Extant tropical
Log DL vs. PC4	0.004908	0.0005815	0.288	232	230	Extant tropical
Log VL vs. PC1	2.04E-05	-0.004327	0.9455	232	230	Extant tropical
Log VL vs. PC2	1.08E-03	-0.003266	0.619	232	230	Extant tropical
Log VL vs. PC3	0.000119	-0.004228	0.8688	232	230	Extant tropical
Log VL vs. PC4	0.0009347	-0.003409	0.6432	232	230	Extant tropical

Table 7. The results of linear regressions comparing Log(10) transformed data against valve measurements and results of the principal components analysis for fossil specimens (N=248).

Variables	Multiple r squared	Adjusted r squared	p Value	n	Df	Dataset
Log Length vs. Log Width	0.1962	0.1929	2.45E-13	248	246	Fossil
Log LW vs PC1	0.8937	0.8932	< 2.2e-16	248	246	Fossil
Log LW vs PC2	0.1409	0.1374	1.02E-09	248	246	Fossil
Log LW vs PC3	0.2145	0.2113	1.37E-14	248	246	Fossil
Log LW vs PC4	0.03534	0.03142	0.002958	248	246	Fossil
Log Length vs. PC1	0.6626	0.6612	< 2.2e-16	248	246	Fossil
Log Length vs. PC2	0.2248	0.2217	2.64E-15	248	246	Fossil
Log Length vs. PC3	0.3059	0.303	< 2.2e-16	248	246	Fossil
Log Length vs. PC4	0.005146	0.001102	0.2604	248	246	Fossil
Log Width vs. PC1	0.005037	0.0009927	0.2655	248	246	Fossil
Log Width vs. PC2	0.07888	0.07514	7.08E-06	248	246	Fossil
Log Width vs. PC3	0.07898	0.07523	6.98E-06	248	246	Fossil
Log Width vs. PC4	0.03946	0.03555	0.001668	248	246	Fossil
Log Ventral Length vs. PC1	0.6577	0.6563	< 2.2e-16	248	246	Fossil
Log Ventral Length vs. PC2	0.2148	0.2116	1.31E-14	248	246	Fossil
Log Ventral Length vs. PC3	0.3155	0.3127	< 2.2e-16	248	246	Fossil
Log Ventral Length vs. PC4	0.005592	0.00155	0.2407	248	246	Fossil
Log Dorsal Length vs. PC1	0.5992	0.5975	< 2.2e-16	248	246	Fossil
Log Dorsal Length vs. PC2	0.2732	0.2703	< 2.2e-16	248	246	Fossil
Log Dorsal Length vs. PC3	0.307	0.3042	< 2.2e-16	248	246	Fossil
Log Dorsal Length vs. PC4	0.0001596	-0.003905	0.8431	248	246	Fossil
Log DV vs. PC1	0.1501	0.1466	2.64E-10	248	246	Fossil
Log DV vs. PC2	0.1693	0.1659	1.50E-11	248	246	Fossil
Log DV vs. PC3	0.01568	0.01168	0.04885	248	246	Fossil
Log DV vs. PC4	0.2488	0.2457	< 2.2e-16	248	246	Fossil
Log DL vs. PC1	0.2372	0.2341	3.55E-16	248	246	Fossil
Log DL vs. PC2	0.01235	0.008333	0.08072	248	246	Fossil
Log DL vs. PC3	0.02973	0.02578	0.006489	248	246	Fossil
Log DL vs. PC4	1.21E-01	0.1175	1.83E-08	248	246	Fossil
Log VL vs. PC1	0.09317	0.08949	9.58E-07	248	246	Fossil
Log VL vs. PC2	0.06126	0.05745	8.16E-05	248	246	Fossil
Log VL vs. PC3	0.01494	0.01093	0.0546	248	246	Fossil
Log VL vs. PC4	2.00E-05	-0.004045	0.9442	248	246	Fossil

Table 8. The results of linear regressions comparing Log(10) transformed data against valve measurements and results of the principal components analysis for extant taxa, comprising both tropical and temperate extant specimens (N=384).

Variables	Multiple r squared	Adjusted r squared	p Value	n	Df	Dataset
Log Length vs. Log Width	0.1688	0.1666	< 2.2e-16	384	382	Extant
Log LW vs PC1	0.8808	0.8805	< 2.2e-16	384	382	Extant
Log LW vs PC2	0.0009515	-0.001664	0.5468	384	382	Extant
Log LW vs PC3	1.94E-06	-0.002616	0.9783	384	382	Extant
Log LW vs PC4	0.002486	-0.0001251	0.3298	384	382	Extant
Log Length vs. PC1	0.2732	0.2713	< 2.2e-16	384	382	Extant
Log Length vs. PC2	0.0615	0.05904	8.61E-07	384	382	Extant
Log Length vs. PC3	0.0003219	-0.002295	0.726	384	382	Extant
Log Length vs. PC4	0.0002947	-0.002322	7.37E-01	384	382	Extant
Log Width vs. PC1	0.2463	0.2444	< 2.2e-16	384	382	Extant
Log Width vs. PC2	0.05252	0.05004	5.71E-06	384	382	Extant
Log Width vs. PC3	3.06E-04	-0.002311	0.7325	384	382	Extant
Log Width vs. PC4	0.001416	-0.001198	0.4622	384	382	Extant
Log Ventral Length vs. PC1	0.144	0.1418	1.34E-14	384	382	Extant
Log Ventral Length vs. PC2	0.03812	0.0356	0.0001178	384	382	Extant
Log Ventral Length vs. PC3	0.0001614	-0.002456	0.804	384	382	Extant
Log Ventral Length vs. PC4	1.47E-05	-0.002603	9.40E-01	384	382	Extant
Log Dorsal Length vs. PC1	0.07888	0.07647	2.16E-08	384	382	Extant
Log Dorsal Length vs. PC2	0.08264	0.08024	9.66E-09	384	382	Extant
Log Dorsal Length vs. PC3	0.006305	0.003704	0.1203	384	382	Extant
Log Dorsal Length vs. PC4	0.00082	-0.001796	5.76E-01	384	382	Extant
Log DV vs. PC1	0.02262	0.02007	0.003129	384	382	Extant
Log DV vs. PC2	0.006542	0.003941	0.1136	384	382	Extant
Log DV vs. PC3	0.005259	2655	0.1561	384	382	Extant
Log DV vs. PC4	1.32E-03	-0.001295	0.4778	384	382	Extant
Log DL vs. PC1	0.1058	0.1034	6.54E-11	384	382	Extant
Log DL vs. PC2	0.01556	0.01298	0.01445	384	382	Extant
Log DL vs. PC3	0.01327	0.01069	0.02395	384	382	Extant
Log DL vs. PC4	0.00628	0.003678	0.1211	384	382	Extant
Log VL vs. PC1	0.003751	0.001143	0.2312	384	382	Extant
Log VL vs. PC2	3.35E-05	-0.002584	0.91	384	382	Extant
Log VL vs. PC3	5.69E-06	-0.002612	0.9629	384	382	Extant
Log VL vs. PC4	0.000233	-0.002384	0.7656	384	382	Extant

Table 9. Results of one way analysis of variance test performed upon the dataset investigation relationships between grouping variables. Post hoc analysis was perfromed with Tukey mulitiple mean comparison at the 95% confidence interval

Data	Dependent Variable	Df	F value	p value	Tukey Post Hoc Adjusted p value from 95% confidence interval	Total n	Specimens (n) within treatment
Age	PC 1	1	26.56	3.43E-07	3.00E-07	632	Fossil=248, Modern=284
Age	PC2	1	4.68	0.0309	0.0308846	632	Fossil=248, Modern 284
Climate	PC 1	2	19.23	7.87E-09	Inset 1	632	Fossil=248, Temperate=152, Tropical=232
Climate	PC2	2	9.638	7.53E-05	Inset 2	633	Fossil=248, Temperate=152, Tropical=232
Continent	PC 1	3	1.1144	3.31E-01	Inset 3	384	North America=173, South America=189, Europe=7,Africa=15
Continent	PC2	3	6.234	3.85E-04	Inset 4	384	North America=173, South America=189, Europe=7,Africa=15
Americas	PC1	1	2.906	8.91E-02	0.0891354	362	North America=173, South America=189
Americas	PC2	1	6.872	0.00913	0.0091264	362	North America=173, South America=189
Fossil Depth	PC1	5	6.031	2.79E-05	Inset 5	248	Box 11=41, Box 13=89, Box 14= 5, Box15.1.131=47, Box 15.1.65= 42, Box 16=24
Fossil Depth	PC2	5	1.828	1.08E-01	Inset 5	248	Box 11=41, Box 13=89, Box 14= 5, Box15.1.131=47, Box 15.1.65= 42, Box 16=24

Table 10. Analysis of variance using procrustes distances comparing the mean (centroid) against all other specimens. Data are presented for 100 and 1000 permutations.

100 Permutations	Df	SS	MS	Rsq	F	Z	p value
Centroid	1	1.0577	1.05771	0.16308	122.76	9.8353	0.01
Residuals	630	5.4282	0.00862				
Total	631	6.4859					
1000 Permutations	Df	SS	MS	Rsq	F	Z	p value
Centroid	1	1.0577	1.05771	0.16308	122.76	28.68	0.001
Residuals	630	5.4282	0.00862				
Total	631	6.4859					

Table 11. Results of disparity measures between extant and fossil specimens. Pairwise distances were compared for 100 and 1000 permutations.

100 Permutations	Procrustes variances for defined groups	Pairwise Absolute Differences between variances	p Values
Fossil	0.003469319	0.008426099	0.01
Modern	0.011895419	0.008426099	0.01
1000 Permutations	Procrustes variances for defined groups	Pairwise Absolute Differences between variances	p Values
Fossil	0.003469319	0.008426099	0.001
Modern	0.011895419	0.008426099	0.001

Table 12. Results of disparity measures between fossil specimens and extant temperate and extant tropical taxa. Pairwise distances were compared for 100 and 1000 permutations.

100 Permutations	Procrustes variances for defined groups			1000 Permutations	Procrustes variances for defined groups		
	Fossil	Temperate	Tropical		Fossil	Temperate	Tropical
	0.004740716	0.012008687	0.015021225		0.00474072	0.01200869	0.015021225
	Pairwise absolute differences between				Pairwise absolute differences between		
	Fossil	Temperate	Tropical		Fossil	Temperate	Tropical
Fossil	0	0.007267971	0.010280509	Fossil	0	0.00726797	0.010280509
Temperate		0	0.003012539	Temperate		0	0.003012539
Tropical			0	Tropical			0
	P-Values				P-Values		
	Fossil	Temperate	Tropical		Fossil	Temperate	Tropical
Fossil	1	0.01	0.01	Fossil	1	0.001	0.001
Temperate		1	0.02	Temperate		1	0.022
Tropical			1	Tropical			1

Table 13. Disparity measures comparing Fossil specimens separated by their section of origin within the sedment core to extant temperate and tropical taxa. Pairwise distances were compared for 1000 permutations.

Procrustes variances for defined groups

11	13	14	15.1.131	15.1.65	16	Temperate	Tropical
0.00593971	0.00457147	0.00259567	0.00417055	0.00443376	0.00542067	0.01200869	0.01502123

Pairwise absolute differences between variances

	11	13	14	15.1.131	15.1.65	16	Temperate	Tropical
11	0	0.00136823	0.00334404	0.00176915	0.00150594	0.00051904	0.0060689	0.00908152
13		0	0.0019758	0.0040092	0.00013771	0.00084919	0.00743721	0.01044975
14			0	0.00157488	0.00183809	0.002825	0.00941302	0.01242556
15.1.131				0	0.00026321	0.00125011	0.00783813	0.01085067
15.1.65					0	0.00986904	0.00757492	0.01058746
16						0	0.00658802	0.00969956
Temperate							0	0.00301254
Tropical								0

p Values

	11	13	14	15.1.131	15.1.65	16	Temperate	Tropical
11	1	0.578	0.573	0.541	0.601	0.889	0.011	0.001
13		1	0.736	0.872	0.952	0.766	0.002	0.001
14			1	0.778	0.724	0.622	0.057	0.026
15.1.131				1	0.907	0.703	0.001	0.001
15.1.65					1	0.76	0.004	0.001
16						1	0.025	0.003
Temperate							1	0.022
Tropical								1

Inset 1. Results of Tukey post hoc test at 95 % confidence interval for ANOVA comparing the scores from PC1 against Climate

Samples Compared	Adjusted p Value	difference	lower	upper
Temperate-Fossil	0.104078	0.01765782	-0.0380134	0.00269776
Tropical-Fossil	0	-0.047362	-0.0654109	-0.029313
Tropical-Temperate	0.0021862	-0.0297041	-0.0503247	-0.0090836

Inset 2. Results of Tukey post hoc test at 95 % confidence interval for ANOVA comparing the scores from PC2 against Climate

Samples Compared	Adjusted p Value	difference	lower	upper
Temperate-Fossil	0.0001637	-0.013467	-0.0212607	-0.0056732
Tropical-Fossil	0.971675	-0.0006716	-0.0075822	0.00623901
Tropical-Temperate	0.0004524	0.01279537	0.00490013	0.02069061

Inset 3. Results of Tukey post hoc test at 95 % confidence interval for ANOVA comparing the scores from PC1 against Continent data

Samples Compared	Adjusted p Value	difference	lower	upper
Europe-Africa	0.9253768	0.02825028	-0.0891656	0.14566619
North America-Africa	0.8622908	0.02094235	-0.0481008	0.08998547
South America-Africa	0.996177	0.0027245	-0.0660851	0.07153406
North America-Europe	0.9975388	-0.0073079	-0.106203	0.09158708
South America-Europe	0.9094054	-0.0255258	-0.1242579	0.07320631
North America-South America	0.3035601	0.01821785	-0.0452083	0.00877263

Inset 4. Results of Tukey post hoc test at 95 % confidence interval for ANOVA comparing the scores from PC2 against Continent data

Samples Compared	Adjusted p Value	difference	lower	upper
Europe-Africa	0.0118486	-5.15E-02	-0.0945973	-0.0083552
North America-Africa	0.714693	-1.04E-02	-0.0357618	0.01495045
South America-Africa	0.9999997	-9.32E-05	-0.0253635	0.02517716
North America-Europe	1.95E-02	4.11E-02	0.00475129	0.07738978
South America-Europe	0.0016533	5.14E-02	0.01512362	0.08764244
North America-South America	0.0378452	1.03E-02	0.00040022	0.02022476

Inset 5. Results of Tukey post hoc test at 95 % confidence interval for ANOVA comparing the scores from PC1 & PC2 against Fossil depth

Samples Compared	Adjusted p Value	
	PC1	PC2
13-11	0.000532	0.6413638
14-11	0.330985	0.2419098
15.1.131-11	0.0001218	0.4820494
15.1.65-11	0.0002176	0.9216061
16-11	0.006808	0.9996179
14-13	0.9992139	0.5756076
15.131-13	0.9180622	0.9961704
15.1.65-13	0.9343422	0.9988145
16-13	0.8469925	0.5952437
15.1.131-14	1	0.7227922
15.1.65-14	1	0.5042526
16-14	0.99993553	0.2059064
15.1.65-15.1.131	1	0.9725776
16-15.1.131	0.9991757	0.4476405
16-15.1.65	0.9991151	0.856151